JAM CM Journal of Applied Mathematics and Computational Mechanics 2025, 24(3), 46-75
www.amcm.pcz.pl p-ISSN 2299-9965
DOI: 10.17512/jamcm.2025.3.04 e-ISSN 2353-0588

# RELIABILITY INFERENCE OF THE INVERTED POWER BURR X DISTRIBUTION UNDER THE HYBRID CENSORING APPROACH WITH APPLICATIONS

***Mohammed Elgarhy[1], Gaber Sallam Salem Abdalla[2], Amal S. Hassan[3]***
***Ehab M. Almetwally[4]***

*[1] Department of Basic Sciences, Higher Institute of Administrative Sciences, Belbeis, AlSharkia Egypt*
*[2] Department of Insurance and Risk Management, College of Business, Imam Mohammad Ibn Saud Islamic University (IMSIU), Riyadh 11432, Saudi Arabia*
*[3] Faculty of Graduate Studies for Statistical Research, Cairo University, Giza, Egypt*
*[4] Department of Mathematics and Statistics, College of Science, Imam Mohammad Ibn Saud Islamic University (IMSIU), Riyadh 11432, Saudi Arabia*
*dr.moelgarhy@gmail.com, jssabdullah@imamu.edu.sa, amal52_soliman@cu.edu.eg*
*emalmetwally@imamu.edu.sa*

Received: 30 March 2025; Accepted: 9 July 2025

**Abstract.** In this study, we provide a novel three-parameter extension of the power Burr X model obtained by the inverse transformation method. The unique model, known as the inverted power Burr X distribution (IP-BXD), is capable of modeling lifespan data with decreasing, increasing, and upside-down patterns, making it ideal for capturing non-monotonic procedures. Explicit formulations are given for numerous statistical measures, such as ordinary moments, incomplete and conditional moments, mean residual lifespan, and mean inactivity time. Furthermore, it can be used quite well in a statistical context. This argument is supported under complete and hybrid censoring samples by an examination of traditional techniques, such as maximum likelihood and maximum product spacing, to estimate the unknown parameters. Additionally, the use of an informative gamma prior under the squared error loss function in the Bayesian estimation approach is clarified. The approximate confidence intervals based on normality approximation as well as the Bayesian credible intervals are determined. We conducted a comparative analysis of different estimates, employing Monte Carlo simulation to evaluate their performance in terms of some accuracy measures. Finally, three real data sets are considered to analyze the usefulness and flexibility of the proposed model in comparison to some other distributions. In addition, we examined these real-world datasets to demonstrate how the suggested distribution could be used in practice using the suggested techniques.

***MSC 2010:*** *62Exx, 62Hxx*
***Keywords:*** *power Burr-X, moments, mean residual lifetime, maximum likelihood estimation, hybrid censoring*

## 1. Introduction

The distribution known as the Burr type *X* distribution (B-XD) was first presented by Burr [1], and it has attracted a significant amount of interest in the academic literature. In the fields of reliability research, predicting the lifetime of random occurrences, health, agriculture, and biology, the B-XD has been a handy tool. In recent years, several authors have conducted research on various aspects of the B-XD. For further information, please refer to Ahmed et al. [2], Surles and Padgett [3], Kundu and Raqab [4], Aludaat et al. [5], and Fayomi et al. [6]. The probability density function (PDF) and cumulative distribution function (CDF) of the B-XD are provided via

$$f(z) = 2\alpha\lambda^2 z e^{-(\lambda z)^2}\left[1-e^{-(\lambda z)^2}\right]^{\alpha-1}, \quad z>0, \tag{1}$$

and

$$G(z) = \left[1-e^{-(\lambda z)^2}\right]^{\alpha}, \quad z>0, \tag{2}$$

where $\alpha>0$ and $\lambda>0$ are the shape and scale parameters, respectively. Utilizing a random variable's power transformation to add a new shape parameter may result in a more flexible model. Usman and Ilyas [7] developed power B-XD (PB-XD) with a shape parameter based on a transformation approach. The CDF and PDF of the PB-XD are provided via

$$G(y) = \left[1-e^{-\left(\lambda y^{\theta}\right)^2}\right]^{\alpha}, \quad y>0, \tag{3}$$

and

$$g(y) = 2\alpha\theta\lambda^2 y^{2\theta-1}\, e^{-\left(\lambda y^{\theta}\right)^2}\left[1-e^{-\left(\lambda y^{\theta}\right)^2}\right]^{\alpha-1}, \quad y>0, \tag{4}$$

respectively, $\theta>0$ is an additional shape parameter.

One of the most popular study topics in probability distributions is determining the inversion of uni-variate probability distributions and their application under the inverse transformation. The study of inverse distributions has resulted in a more comprehensive understanding of standard distributions and has added more flexibility for the purpose of fitting data. Inverted distributions have a wide variety of applications, including finding solutions to issues in the fields of survey sampling, life testing, econometrics, engineering sciences, biological sciences and medical research. For example, the inverted Kumaraswamy by Abd AL-Fattah et al. [8], estimation of parameters for inverse power Ailamujia and truncated inverse Power Ailamujia distributions based on progressive Type-II censoring Scheme by ElGazar et al. [9], new hybrid Weibull-inverse Weibull distribution by Noori et al. [10], inverted exponentiated Lomax by Hassan and Mohamed [11], inverted weighted Lindley by Ramos

et al. [12], inverted Pareto by Guo and Gui [13], inverted Lindley by Sharma et al. [14], inverted power Lindley by Barco et al. [15], inverse Sushila by Adetunji et al. [16], inverted Akash by Okereke et al. [17], inverted exponentiated Weibull by Lee et al. [18], inverted power Lomax by Hassan and Abd-Alla [19], inverted power Akash by Enogwe et al. [20], inverted xgamma by Yadav et al. [21], inverted Nadarajah-Haghighi by Tahir et al. [22], inverted Topp-Leone by Hassan et al. [23], inverted power Cauchy by Sapkota and Kumar [24], inverted Hamza by Frank et al. [25], bivariate Fréchet distribution by Almetwally and Muhammed [26], inverted Shanker by Pokalas et al. [27], inverted power modified Chris-Jerry by Awajan et al. [28], inverted Weibull generator by Abdelall et al. [29], inverted Nakagami-m by Louzada et al. [30], inverted Maxwell by Omar et al. [31], inverted power Ramos--Louzada by Al Mutairi et al. [32], inverted unit Teissier by Alsadat et al. [33], inverse power Zeghdoudi by Elbatal et al. [34], inverted power XLindley by Hassan et al. [35] distributions, etc.

In this study, we introduce a novel three-parameter inverted distribution based on the PB-XD, which referred to the inverted PB-XD (IPB-XD), derived through an inverse transformation technique. We investigated the IPB-XD for the subsequent justifications:

- The IPB-XD can model increasing, decreasing or upside-down accommodating different patterns of failure rates. It is particularly suitable for fitting skewed data that may not be adequately modeled by other common distributions.
- A number of structural features are explained, including explicit formulas for the mean residual lifespan (MRL), moments of residual life function (RLF), quantile function (QF), moments of reversed residual life function (RRLF), ordinary moments, incomplete moments (IMs), and conditional moments (CMs). These characteristics offer a thorough comprehension of the behavior of the model.
- It is critical to identify the optimal estimation method for the IPB-XD parameters. In light of this, three different estimating techniques, including maximum likelihood (ML), maximum product spacing (MPS), and Bayesian approaches are investigated under complete and hybrid censoring sampling.
- Bayesian estimators (BEs) of the IPB-XD parameters, reliability function (RF), and hazard rate function (HRF), under the squared error loss function, is determined using gamma prior distributions. Additionally, approximate confidence intervals (ACIs) and highest posterior density (HPD) credible intervals are generated.
- To address the computational challenges associated with BEs and HPD intervals, we employ the Markov chain Monte Carlo (MCMC) approximation method. Monte Carlo simulation research was carried out, taking into account

varied sample sizes, to assess the efficacy of different estimates under various hybrid censoring scenarios.

- The IPB-XD consistently provides superior results in modeling lifetime data compared to competing distributions, as evidenced by its successful application to two real-world datasets (see Section 6).

The following is the order of the article: The construction of the innovative distribution along with some of its graphical representation are presented in Section 2. The novel distribution's attributes are shown in Section 3. The description of the hybrid censoring scheme along with the ML estimators (MLEs), MPS estimators (MLEs), and BEs of the IPB-XD parameters, RF and HRF, is given in Section 4. The Monte Carlo simulation method technique is presented in Section 5. To assess the IPB-XD's flexibility and practical usefulness compared to other models, Section 6 offers two real-world data sets.

## 2. The IPB-XD description

This section introduces a three-parameter model called the IPB-XD as a new extended version of the PB-XD. Expressions of the PDF, CDF, RF, HRF, and cumulative HRF (CHRF) are presented. Also, graphical representation and 3D plots for the PDF, CDF, RF, and HRF are provided.

Suppose that the random variably $Y$ has the CDF of equation (3), then $X = \frac{1}{Y}$ follows the IPB-XD. The CDF for the IPB-XD is available via

$$F(x;\Psi) = 1 - \left[1 - e^{-\lambda^2 x^{-2\theta}}\right]^{\alpha}, \quad x > 0, \tag{5}$$

and $F(x;\Psi) = 0$ for $x \leq 0$, where $\theta, \alpha > 0$ are shape parameters, $\lambda > 0$ is the scale parameter, and $\Psi = (\alpha, \lambda, \theta)^T$ is the set of parameters. The corresponding PDF is defined by

$$f(x;\Psi) = 2\alpha\theta\lambda^2 x^{-2\theta-1} e^{-\lambda^2 x^{-2\theta}} \left[1 - e^{-\lambda^2 x^{-2\theta}}\right]^{\alpha-1}, \quad x > 0, \tag{6}$$

and $f(x;\Psi) = 0$ for $x \leq 0$. For $\theta = 1$ in equation (5), the IPB-XD reduces to the inverted exponentiated Rayleigh distribution (inverted Burr X) (see Ghitany et al. [36]). For $\theta = 1$, and $\alpha = 1$ in equation (5), the IPB-XD reduces to the inverted Rayleigh distribution (see Voda [37]).

The RF, HRF, and CHRF of the IPB-XD are given, respectively by:

$$R(x;\Psi) = \left[1 - e^{-\lambda^2 x^{-2\theta}}\right]^{\alpha},$$

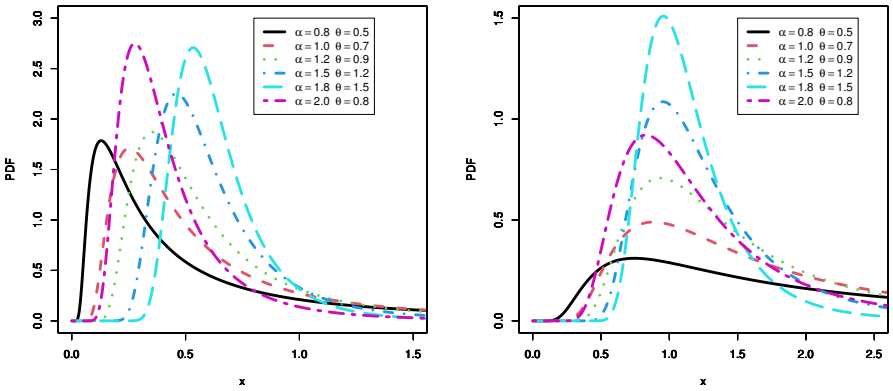


Fig. 1. Graphs of the PDF for the IPB-XD at $\lambda = 0.5$ and 1.2

and $R(x;\Psi) = 1$ for $x \leq 0$,

$$h(x;\Psi) = \frac{2\alpha\theta\lambda^2 x^{-2\theta-1} e^{-\lambda^2 x^{-2\theta}}}{1 - e^{-\lambda^2 x^{-2\theta}}},$$

and $h(x;\Psi) = 0$ for $x \leq 0$,

$$H(x;\Psi) = -\alpha \log\left[1 - e^{-\lambda^2 x^{-2\theta}}\right],$$

and $H(x;\Psi) = 0$ for $x \leq 0$, respectively.

Figures 1 and 5 represent different PDF graphs and 3D plots for the IPB-XD for different values of the parameters. As seen by the visual representation, the IPB-XD can take different uni-modals and asymmetric patterns. Figure 2 graphically illustrates the increasing CDF and decreasing RF of the IPB-XD for selected parameter values. This behavior is also visually evident in the 3D plots presented in Figure 3. The IPB-XD HRF is versatile, as shown in Figures 4 and 5, showing how it can display increasing, decreasing, and upside-down shapes through various HRF graphs and 3D plots for the parameters provided.

## 3. Characteristic analysis of the IPB-XD

In this section, we present some important statistical and mathematical measures for the IPB-XD model, such as, QF, ordinary moments, MRL, mean inactivity time (MIT), RLF, QF, RRLF, IMs, and CMs.

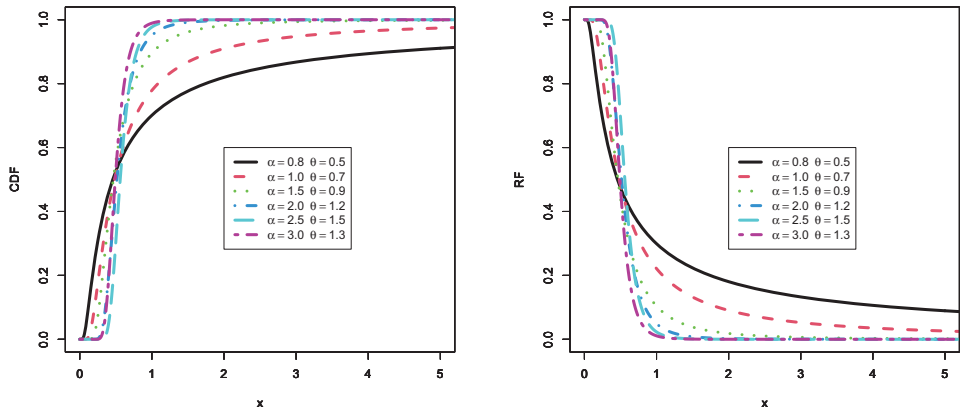


Fig. 2. Graphs of the CDF and RF for the IPB-XD at $\lambda = 0.5$

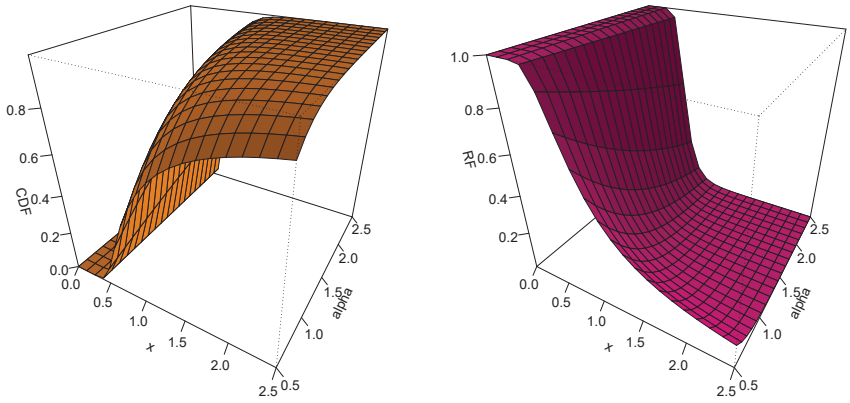


Fig. 3. 3D graphs of the CDF and RF for the IPB-XD at $\lambda = 0.5$ and $\theta = 1.5$

### 3.1. Quantile function

QFs are used in theoretical aspects, statistical applications and Monte Carlo methods. Monte Carlo simulations employ QFs to produce simulated random variables for classical and new continuous distributions. The $p$-th QF of IPB-XD can be obtained by inverting equation (5) as follows:

$$x_p = Q(p) = \left\{ \frac{1}{\lambda^2} \log \left( \frac{1}{1-(1-p)^{\frac{1}{\alpha}}} \right) \right\}^{\frac{-1}{2\theta}},$$

where $p \in (0,1)$. One of the earliest skewness measures to be suggested is the Bowley skewness (Kenney and Keeping [38]) defined by:

$$SK = \frac{Q(\frac{3}{4}) + Q(\frac{1}{4}) - 2Q(\frac{1}{2})}{Q(\frac{3}{4}) - Q(\frac{1}{4})}.$$

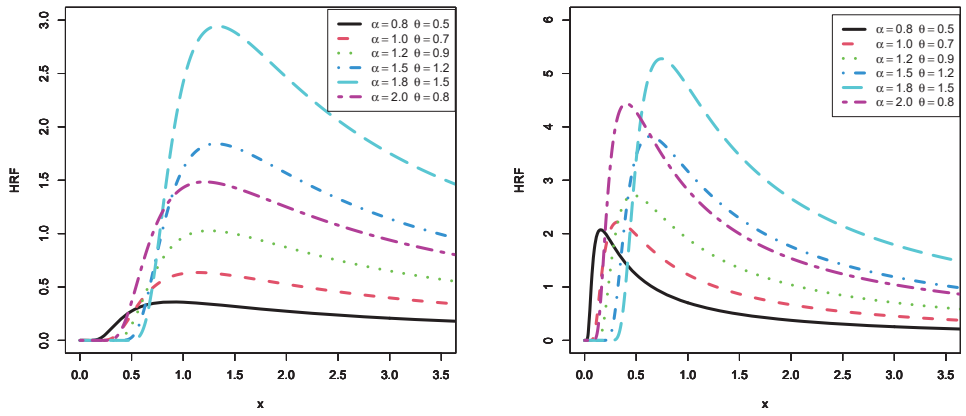


Fig. 4. Graphs of the HRF for the IPB-XD at $\lambda = 0.5$ and 1.2

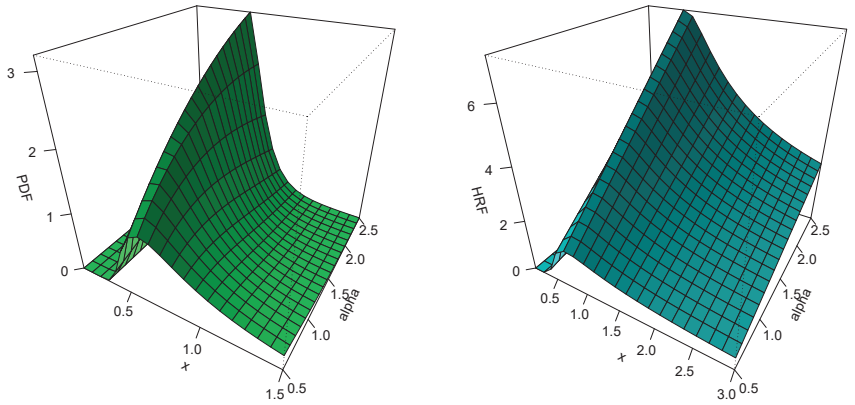


Fig. 5. 3D graphs of the PDF and HRF for the IPB-XD at $\lambda = 0.5$ and $\theta = 1.5$

On the other hand, the Moors kurtosis (Moors [39]) based on quantiles is given by:

$$KU = \frac{Q(\frac{7}{8}) - Q(\frac{5}{8}) + Q(\frac{3}{8}) - Q(\frac{1}{8})}{Q(\frac{6}{8}) - Q(\frac{2}{8})},$$

where $Q(\cdot)$ represents the QF. The measures $SK$ and $KU$ are less sensitive to outliers and they exist even for distributions without moments. For symmetric unimodal distributions, positive kurtosis indicates heavy tails and peakedness relative to the normal distribution, whereas negative kurtosis indicates light tails and flatness. For the normal distribution, $SK = KU = 0$.

### 3.2. Some measures of moments

In statistical analysis, a moment examination is crucial for understanding the properties of any lifetime distribution. It provides a numerical way to model the distribu-

tion's characteristics by identifying the behavior of key parameters. This includes mean, variance, skewness, and kurtosis coefficients. The $r$-th moment of IPB-XD is obtained as the following:

$$\mu_r^{'} = \int_0^{\infty} x^r f(x;\Psi)dx = 2\alpha\theta\lambda^2 \int_0^{\infty} x^{r-2\theta-1} e^{-\lambda^2 x^{-2\theta}} \left[1 - e^{-\lambda^2 x^{-2\theta}}\right]^{\alpha-1} dx. \quad (7)$$

If $|z| < 1$ and $b > 0$ is a real non-integer, the power series hold

$$(1-z)^{b-1} = \sum_{i=0}^{\infty} (-1)^i \binom{b-1}{i} z^i.$$

Therefore, by using the previous expansion in equation (7), the $r$-th moment becomes as follows

$$\mu_r^{'} = 2\alpha\theta\lambda^2 \sum_{i=0}^{\infty} (-1)^i \binom{\alpha-1}{i} \int_0^{\infty} x^{r-2\theta-1} e^{-(i+1)\lambda^2 x^{-2\theta}} dx. \quad (8)$$

Using the transformation $y = (i+1)\lambda^2 x^{-2\theta}$, in equation (8), and after some integral manipulations, the $r$-th moment reduces to

$$\mu_r^{'} = \alpha\lambda^{\frac{r}{\theta}} \sum_{i=0}^{\infty} (-1)^i \binom{\alpha-1}{i} \frac{\Gamma(1-\frac{r}{2\theta})}{(i+1)^{1-\frac{r}{2\theta}}}, r < 2\theta. \quad (9)$$

The moment generating function of the IPB-XD, based on equation (9), can be expressed as:

$$M_X(t) = \sum_{i,j=0}^{\infty} \alpha\lambda^{\frac{r}{\theta}} (-1)^i \binom{\alpha-1}{i} \frac{t^r}{r!} \frac{\Gamma(1-\frac{r}{2\theta})}{(i+1)^{1-\frac{r}{2\theta}}}, r < 2\theta.$$

A number of statistical metrics depend heavily on incomplete moments. The $s$-th IM of the IPB-XD distribution is given by:

$$\begin{aligned} \varkappa_s(t) &= E(X^s \mid X < t) = \int_0^t x^s f(x;\Psi)dx \\ &= 2\alpha\theta\lambda^2 \sum_{i=0}^{\infty} (-1)^i \binom{\alpha-1}{i} \int_0^t x^{r-2\theta-1} e^{-(i+1)\lambda^2 x^{-2\theta}} dx \\ &= \alpha\lambda^{\frac{s}{\theta}} \sum_{i=0}^{\infty} (-1)^i \binom{\alpha-1}{i} \frac{\Gamma(1-\frac{s}{2\theta}, (i+1)\lambda^2 t^{-2\theta})}{(i+1)^{1-\frac{s}{2\theta}}}. \end{aligned} \quad (10)$$

where $\Gamma(s,t) = \int_t^{\infty} x^{s-1} e^{-x} dx$ is the upper incomplete gamma function. The Lorenz and Bonferroni curves, which are helpful in science, engineering, economics, and demography, are estimated using the incomplete moment. The mathematical expression for these numbers are the Lorenz $L(t) = \varkappa_1(t)/\mu'_1$, where $\varkappa_1(t)$ is obtained

from equation (10) by putting $s = 1$, while the Bonferroni curves, represented by $B(t) = L(t)/F(t;\Psi)$.

For the IPB-XD model, the CM defined by $E(X^s \mid X > t)$, which is represented as

$$E(X^s \mid X > t) = \frac{1}{R(t;\Psi)}\eta_s(t),$$

where

$$\begin{aligned}\eta_s(t) &= \int_t^\infty x^s f(x;\Psi)dx = 2\alpha\theta\lambda^2 \sum_{i=0}^{\infty}(-1)^i\binom{\alpha-1}{i}\int_t^\infty x^{r-2\theta-1}e^{-(i+1)\lambda^2 x^{-2\theta}}dx \\ &= \alpha\lambda^{\frac{s}{\theta}}\sum_{i=0}^{\infty}(-1)^i\binom{\alpha-1}{i}\frac{\gamma(1-\frac{s}{2\theta},(i+1)\lambda^2 t^{-2\theta})}{(i+1)^{1-\frac{s}{2\theta}}}, \qquad (11)\end{aligned}$$

and $\gamma(s,t) = \int_0^t x^{s-1}e^{-x}dx$ is the lower incomplete gamma function.

### 3.3. Moments of residual lives

Let a component's operational lifespan be represented by the random variable $X$. The residual lifetime, defined as the time remaining until failure given that the component is still functioning at time $t$, can be expressed as the conditional random variable $X - t|X > t$. The $n$-th order moment of RLF of random variable $X$ is given by:

$$\psi_n(t) = E((X-t)^n \mid X > t) = \frac{1}{R(t;\Psi)}\int_t^\infty (x-t)^n f(x;\Psi)dx, \quad n \geq 1.$$

Using PDF (6) and applying the binomial expansion of the term $(x-t)^n$ into the above formula gives

$$\begin{aligned}\psi_n(t) &= \frac{1}{R(t;\Psi)}\sum_{d=0}^{n}(-t)^{n-d}\binom{n}{d}\int_t^\infty x^n f(x;\Psi)dx \\ &= \frac{\alpha\lambda^{\frac{s}{\theta}}}{R(t;\Psi)}\sum_{i=0}^{\infty}\sum_{d=0}^{n}(-1)^i(-t)^{n-d}\binom{\alpha-1}{i}\binom{n}{d}\frac{\gamma(1-\frac{s}{2\theta},(i+1)\lambda^2 t^{-2\theta})}{(i+1)^{1-\frac{s}{2\theta}}}. \qquad (12)\end{aligned}$$

The MRL plays a very important role in reliability, survival analysis, actuarial sciences, economics, and social sciences for characterizing lifetime distributions. It also plays an important role in repair and replacement strategies and summarizes the entire residual life function. For IPB-XD, the MRL is obtained by setting $n = 1$ in equation (12) as follows:

$$\begin{aligned}\psi_1(t) &= E((X-t) \mid X>t) = \frac{1}{R(t;\Psi)}\int_t^{\infty} xf\,(x;\Psi)dx - t \\ &= \frac{\alpha\lambda^{\frac{1}{\theta}}}{R(t;\Psi)}\sum_{i=0}^{\infty}(-1)^i\binom{\alpha-1}{i}\frac{\gamma(1-\frac{1}{2\theta},(i+1)\lambda^2 t^{-2\theta})}{(i+1)^{1-\frac{1}{2\theta}}} - t.\end{aligned}$$

### 3.4. Moments of reversed residual lives

In reliability theory, the RRLF describes the additional time a component remains inactive after failing at time $t$. The conditional random variable $t-X|X<t$ represents the elapsed time since the component's failure, given that it failed before or at time $t$. The $r$-th moment of RRLF can be obtained by the following formula

$$\xi_r(t) = E((t-X)^r \mid X \le t) = \frac{1}{F(t;\Psi)}\int_0^t (t-x)^r f(x;\Psi)dx.$$

Using PDF (6) and applying the binomial expansion for the term $(t-x)^r$ into the above formula, we get

$$\begin{aligned}\xi_r(t) &= \frac{1}{F(t;\Psi)}\sum_{d=0}^{r}(-t)^{r-d}\binom{r}{d}\int_0^t x^r f(x;\Psi)dx \\ &= \frac{\alpha\lambda^{\frac{s}{\theta}}}{F(t;\Psi)}\sum_{i=0}^{\infty}\sum_{d=0}^{n}(-1)^i(-t)^{n-d}\binom{\alpha-1}{i}\binom{n}{d}\frac{\Gamma(1-\frac{s}{2\theta},(i+1)\lambda^2 t^{-2\theta})}{(i+1)^{1-\frac{s}{2\theta}}}. \quad (13)\end{aligned}$$

The MIT is obtained by setting $r=1$ in equation (13) as follows:

$$\begin{aligned}\xi_1(t) &= E(t-X \mid X \le t) = t - \frac{1}{F(t;\Psi)}\int_0^t xf(x;\Psi)dx \\ &= t - \frac{\alpha\lambda^{\frac{1}{\theta}}}{F(t;\Psi)}\sum_{i=0}^{\infty}(-1)^i\binom{\alpha-1}{i}\frac{\Gamma(1-\frac{1}{2\theta},(i+1)\lambda^2 t^{-2\theta})}{(i+1)^{1-\frac{1}{2\theta}}}.\end{aligned}$$

## 4. Statistical inference under hybrid censoring

This section provides details on the characteristics of hybrid censoring samples used in the study. Three different estimating techniques, including ML, MPS, and Bayesian are suggested to obtain the point estimators of the parameters $\alpha,\theta,\lambda$, as well as RF and HRF of the IPB-XD. Interval estimators, including ACI as well as the HPD credible intervals, are produced. More papers used hybrid censoring samples as: Al Mutairi et al. [40] discussed Bayesian and non-Bayesian inference for inverse Weibull model based on joint censoring. Haj Ahmad et al. [41] obtained statistical analysis of alpha power inverse Weibull distribution. Almetwally et al. [42] discussed estimation and prediction for alpha-power Weibull distribution.

### 4.1. Hybrid censoring description

A popular experimental design known as hybrid censoring terminates the test at a predefined number of failures $r$ or a specified time $T$. We consider $n$ test units in this investigation, whose lifetime items $x_{1:n} < x_{2:n} < \cdots < x_{n:n}$ are distributed with the PDF $f(x;\Psi)$, where $\Psi$ is a vector of unknown parameters. Three types of observations are feasible as a result of the experiment stopping at $\tau = \min(T; x_{r:n})$. The observed lifetime under this censorship can therefore be classified as:

- **Type-I censored**: $x_{1:n} < x_{2:n} < \cdots < x_{d:n}$, if $d < r$ and $x_{d:n} < T < x_{d+1:n}$.
- **Type- II censored**: $x_{1:n} < x_{2:n} < \cdots < x_{r:n}$, if $x_{r:n} < T$.
- **Complete sample**: $x_{1:n} < z_{2:n} < \cdots < x_{n:n}$, if $x_{n:n} < T$ and $n = r$.

Note that $d$ represents the number of failures observed before the pre-specified time $T$. The likelihood function for a censored hybrid sample $x_{1:n} < x_{2:n} < \cdots < x_{d:n}$, following a distribution with PDF $f(x;\Psi)$ and CDF $F(x;\Psi)$, is defined as follows:

$$L(\Psi) \propto [1 - F(\tau;\Psi)]^{n-d} \prod_{i=1}^{d} f(x_i;\Psi). \tag{14}$$

For further details regarding the hybrid censoring sample (see Balakrishnan and Kundu [43]).

### 4.2. Maximum likelihood method

An effective technique for estimating the parameter $\Psi$, where $\Psi = (\alpha, \theta, \lambda)^T$, RF and HRF of the IPB-XD is the ML estimation approach. Let $x_1, x_2, ..., x_n$ be a hybrid censored sample observed form the PDF (6) and CDF (5), then the likelihood function for the set of parameters and observed samples is determined based on equation (14) as follows:

$$l(\underline{\boldsymbol{x}}|\Psi) = (2\alpha\theta\lambda^2)^n \left[1 - e^{-\lambda^2\tau^{-2\theta}}\right]^{\alpha(n-d)} \prod_{k=1}^{n} x_k^{-2\theta-1} \left[1 - e^{-\lambda^2 x_k^{-2\theta}}\right]^{\alpha-1} e^{-\lambda^2 x_k^{-2\theta}}. \tag{15}$$

The logarithm of equation (15) is as follows:

$$l^* \propto n\log(\alpha\theta\lambda^2) + \alpha(n-d)\log\left[1 - e^{-\lambda^2\tau^{-2\theta}}\right] + \sum_{k=1}^{n}(\alpha-1)\log\left[1 - e^{-\lambda^2 x_k^{-2\theta}}\right] - (2\theta+1)\sum_{k=1}^{n}\log x_k - \lambda^2 \sum_{k=1}^{n} x_k^{-2\theta}. \tag{16}$$

The MLEs $\hat{\alpha}, \hat{\theta}$, and $\hat{\lambda}$ are obtained after differentiating equation (16) with respect to the parameters $\alpha, \theta$, and $\lambda$ then equating them with zero

$$\frac{\partial l^*}{\partial \alpha} = \frac{n}{\alpha} + (n-d)\log\left[1-e^{-\lambda^2\tau^{-2\theta}}\right] + \sum_{k=1}^{n}\log\left[1-e^{-\lambda^2 x_k^{-2\theta}}\right] = 0,$$

$$\frac{\partial l^*}{\partial \theta} = \frac{n}{\theta} - \frac{2\alpha(n-d)\lambda^2\tau^{-2\theta}\log\tau}{e^{\lambda^2\tau^{-2\theta}}-1} - (\alpha-1)\sum_{k=1}^{n}\frac{x_k^{-2\theta}\lambda^2\log x_k}{e^{\lambda^2 x_k^{-2\theta}}-1} - 2\sum_{k=1}^{n}\log x_k + 2\lambda^2\sum_{k=1}^{n}x_k^{-2\theta}\log x_k = 0,$$

and

$$\frac{\partial l^*}{\partial \lambda} = \frac{2n}{\lambda} + \frac{2\lambda\alpha(n-d)\tau^{-2\theta}}{e^{\lambda^2\tau^{-2\theta}}-1} + \sum_{k=1}^{n}\frac{2(\alpha-1)\lambda x_k^{-2\theta}}{e^{\lambda^2 x_k^{-2\theta}}-1} - 2\lambda\sum_{k=1}^{n}x_k^{-2\theta} = 0.$$

A strong and effective tool for computing the MLEs $\hat{\alpha}, \hat{\theta}$, and $\hat{\lambda}$ using the Newton--Raphson approach is the R'maxLik' package. This software is commonly employed in statistical analysis as it simplifies the ML estimation process.

Furthermore, the MLEs of RF and HRF represented by $\hat{R}$ and $\hat{H}$ are obtained based on the invariance property as mentioned below:

$$\hat{R} = 1 - e^{-\hat{\lambda}^2 t^{-2\hat{\theta}}},$$

and

$$\hat{H} = \frac{2\hat{\alpha}\,\hat{\theta}\,\hat{\lambda}^2 t^{-2\hat{\theta}-1}}{e^{\hat{\lambda}^2 t^{-2\hat{\theta}}}-1}.$$

The ACI of parameters $\alpha, \theta$, and $\lambda$ are created by using the asymptotic distribution of MLEs $\hat{\alpha}, \hat{\theta}$, and $\hat{\lambda}$. It is difficult to obtain the Fisher information matrix (FIM), so its observed value is obtained $I(\Psi) = I_{i_1,i_2} = \left[\partial^2 l^*(\Psi)\Big/(\partial\Psi_{i_1}\partial\Psi_{i_2})\right], i_1, i_2 = 1,2,3,$ $\Psi = (\alpha, \theta, \lambda)$, and $I^{-1}(\Psi)$ is the inverse of FIM.

Thus, the $(1-\varepsilon)\%$ ACIs for $\Psi = (\alpha, \theta, \lambda)$, are given by $\hat{\Psi} \pm Z_{\varepsilon/2}\sqrt{\widehat{\mathrm{var}}(\hat{\Psi})}$, where $Z_{\varepsilon/2}$ denoted the upper $(\varepsilon/2)$ percent point of standard normal distribution, where $Z_{\varepsilon/2}$ is the upper $\varepsilon/2$ quantile of $N(0,1)$.

To construct ACIs for the RF and HRF, we need to estimate their variances. The delta method, as described by Greene [44], provides an approximation for these variances. The approximate variances of $\hat{R}$ and $\hat{H}$ are calculated as follows:

$$\mathrm{var}(\hat{R}) = [\delta_1\hat{R}]^T[I^{-1}(\Psi)][\delta_1\hat{R}], \text{ and } \mathrm{var}(\hat{H}) = [\delta_2\hat{H}]^T[I^{-1}(\Psi)][\delta_2\hat{H}],$$

$$\text{where } \delta_1\hat{R} = \left(\frac{\partial R}{\partial\alpha}, \frac{\partial R}{\partial\theta}, \frac{\partial R}{\partial\lambda}\right), \text{ and } \delta_2\hat{H} = \left(\frac{\partial H}{\partial\alpha}, \frac{\partial H}{\partial\theta}, \frac{\partial H}{\partial\lambda}\right).$$

Thus, the two-sided $100(1-\varepsilon)\%$ ACI of $\hat{R}$ and $\hat{H}$ can be constructed as follows:

$$\hat{R} \pm Z_{\varepsilon/2}\sqrt{\widehat{\mathrm{var}}(\hat{R})}, \quad \hat{H} \pm Z_{\varepsilon/2}\sqrt{\widehat{\mathrm{var}}(\hat{H})}.$$

### 4.3. Maximum product spacing method

In some situations, the MPS technique offers multiple benefits over the typical ML method, making it a strong substitute. The research conducted by Cheng and Amin [45] offers significant understanding of the consistency and asymptotic characteristics of MPS estimators (MPSEs). According to their research, MPSEs can provide comparable or even better efficiency than MLEs, making them a viable alternative.

Let $x_{(1)}, x_{(2)}, ..., x_{(n)}$ be an ordered random sample of size $n$ drawn from the IPB-XD. The uniform spacings are defined as the differences

$$D_i(\Psi) = F\left(x_{(i)};\Psi\right) - F\left(x_{(i-1)};\Psi\right), \quad i = 1,2,...,n+1,$$

where $F\left(x_{(0)};\Psi\right) = 0$, $F\left(x_{(n+1)};\Psi\right) = 1$, such that $\sum_{i=1}^{n+1} D_i(\Psi) = 1$.

For hybrid censored samples, the following is the general MPS expression

$$l_1(\Psi) \propto [1 - F(\tau;\Psi)]^{n-d} \prod_{i=1}^{n+1} [D_i(\Psi)].$$

The MPSEs of IPB-XD parameters based on hybrid censored samples are obtained by maximizing the following function:

$$\ln l_1(\Psi) = \alpha(n-d)\ln\left[1 - e^{-\lambda^2\tau^{-2\theta}}\right] + \sum_{i=1}^{n+1} \ln\left[\left[1 - e^{-\lambda^2 x_{(i-1)}^{-2\theta}}\right]^{\alpha} - \left[1 - e^{-\lambda^2 x_{(i)}^{-2\theta}}\right]^{\alpha}\right]. \tag{17}$$

The MPSE $\hat{\alpha}_1, \hat{\theta}_1$, and $\hat{\lambda}_1$ of the IPB-XD parameters be obtained by solving the nonlinear equations with respect to $\alpha, \theta$, and $\lambda$ instead of using equation (17)

$$\frac{\partial \ln l_1(\Psi)}{\partial \alpha} = (n-d)\ln\left[1 - e^{-\lambda^2\tau^{-2\theta}}\right]$$
$$+ \sum_{i=1}^{n+1} \frac{\left[1 - e^{-\lambda^2 x_{(i-1)}^{-2\theta}}\right]^{\alpha} \ln\left[1 - e^{-\lambda^2 x_{(i-1)}^{-2\theta}}\right] - \left[1 - e^{-\lambda^2 x_{(i)}^{-2\theta}}\right]^{\alpha} \ln\left[1 - e^{-\lambda^2 x_{(i)}^{-2\theta}}\right]}{\left[1 - e^{-\lambda^2 x_{(i-1)}^{-2\theta}}\right]^{\alpha} - \left[1 - e^{-\lambda^2 x_{(i)}^{-2\theta}}\right]^{\alpha}} = 0,$$

$$\frac{\partial \ln l_1(\Psi)}{\partial \theta} = -\frac{2\alpha(n-d)\lambda^2\tau^{-2\theta}\ln\tau}{e^{\lambda^2\tau^{-2\theta}}-1} - \sum_{i=1}^{n+1}\frac{2\alpha\lambda^2 x_{(i-1)}^{-2\theta}e^{-\lambda^2 x_{(i-1)}^{-2\theta}}\left[1-e^{-\lambda^2 x_{(i-1)}^{-2\theta}}\right]^{\alpha-1}\ln x_{(i-1)}}{\left[1-e^{-\lambda^2 x_{(i-1)}^{-2\theta}}\right]^{\alpha}-\left[1-e^{-\lambda^2 x_{(i)}^{-2\theta}}\right]^{\alpha}}$$
$$+\sum_{i=1}^{n+1}\frac{2\alpha\lambda^2 x_{(i)}^{-2\theta}e^{-\lambda^2 x_{(i)}^{-2\theta}}\left[1-e^{-\lambda^2 x_{(i)}^{-2\theta}}\right]^{\alpha-1}\ln x_{(i)}}{\left[1-e^{-\lambda^2 x_{(i-1)}^{-2\theta}}\right]^{\alpha}-\left[1-e^{-\lambda^2 x_{(i)}^{-2\theta}}\right]^{\alpha}} = 0,$$

and

$$\frac{\partial \ln l_1(\Psi)}{\partial \lambda} = \frac{2\lambda\alpha(n-d)\tau^{-2\theta}}{e^{\lambda^2\tau^{-2\theta}}-1}$$
$$+\sum_{i=1}^{n+1}\frac{2\alpha\lambda\left[1-e^{-\lambda^2 x_{(i-1)}^{-2\theta}}\right]^{\alpha-1}x_{(i-1)}^{-2\theta}e^{-\lambda^2 x_{(i-1)}^{-2\theta}} - 2\alpha\lambda\left[1-e^{-\lambda^2 x_{(i)}^{-2\theta}}\right]^{\alpha-1}x_{(i)}^{-2\theta}e^{-\lambda^2 x_{(i)}^{-2\theta}}}{\left[\left[1-e^{-\lambda^2 x_{(i-1)}^{-2\theta}}\right]^{\alpha}-\left[1-e^{-\lambda^2 x_{(i)}^{-2\theta}}\right]^{\alpha}\right]} = 0.$$

The MPSE $\hat{R}_1(t)$ and $\hat{H}_1(t)$ are obtained based on the invariance property as mentioned below:

$$\hat{R}_1(t) = 1-e^{-\hat{\lambda}_1^2 t^{-2\hat{\theta}_1}},$$

and

$$\hat{H}_1(t) = \frac{2\hat{\alpha}_1\hat{\theta}_1\hat{\lambda}_1^2 t^{-2\hat{\theta}_1-1}}{e^{\hat{\lambda}_1^2 t^{-2\hat{\theta}_1}}-1}.$$

Furthermore, the MPS approach is used to generate the ACIs of the parameters $\alpha, \theta, \lambda$, RF and HRF. This procedure is comparable to the one outlined in the preceding subsection, except that the MLEs are replaced with the MPSEs.

### 4.4. Bayesian estimation method

Here BEs for the IPB-XD's parameters, $R(t)$ and $H(t)$ under hybrid censoring are explored. This assumes that the parameters $\alpha, \theta$, and $\lambda$ of the IPB-XD have independent gamma prior distributions. That is $\alpha \sim$ Gamma $(c_1, d_1)$, $\theta \sim$ Gamma $(c_2, d_2)$, and $\lambda \sim$ Gamma $(c_3, d_3)$, then the joint prior of $\alpha, \theta$, and $\lambda$, is as follows:

$$\mathrm{A}(\Psi) \propto \alpha^{c_1-1}\theta^{c_2-1}\lambda^{c_3-1}e^{-(d_1\alpha+d_2\theta+d_3\lambda)}, \tag{18}$$

where, $c_i$ and $d_i, i = 1,2,3$ are the hyper-parameters. By combining the joint prior given in equation (18) and the LF given in equation (15), we can derive the joint posterior density function

$$l\left(\Psi\middle|\underline{\underline{\boldsymbol{x}}}\right) \propto \alpha^{c_1+n-1}\theta^{c_2+n-1}\lambda^{c_3+2n-1}e^{-(d_1\alpha+d_2\theta+d_3\lambda)}\left[1-e^{-\lambda^2\tau^{-2\theta}}\right]^{\alpha(n-d)} \times\prod_{k=1}^{n}x_k^{-2\theta-1}\left[1-e^{-\lambda^2 x_k^{-2\theta}}\right]^{\alpha-1}e^{-\lambda^2 x_k^{-2\theta}}.$$

The marginal posterior densities of the $\alpha,\theta,\lambda$, RF and HRF are provided as follows

$$l\left(\alpha\middle|\lambda,\theta,\underline{\underline{\boldsymbol{x}}}\right) \propto \alpha^{c_1+n-1}e^{-\alpha\left(d_1+\sum_{k=1}^{n}\ln\left[1-e^{-\lambda^2 x_k^{-2\theta}}\right]\right)}\left[1-e^{-\lambda^2\tau^{-2\theta}}\right]^{\alpha(n-d)}\prod_{k=1}^{n}x_k^{-2\theta-1}e^{-\lambda^2 x_k^{-2\theta}}, \tag{19}$$

$$l\left(\theta\middle|\alpha,\lambda,\underline{\underline{\boldsymbol{x}}}\right) \propto \theta^{c_2+n-1}e^{-(d_2\theta+\sum_{k=1}^{n}\lambda^2 x_k^{-2\theta})}\left[1-e^{-\lambda^2\tau^{-2\theta}}\right]^{\alpha(n-d)}\prod_{k=1}^{n}x_k^{-2\theta-1}\left[1-e^{-\lambda^2 x_k^{-2\theta}}\right]^{\alpha-1}, \tag{20}$$

$$l\left(\lambda\middle|\alpha,\theta,\underline{\underline{\boldsymbol{x}}}\right) \propto \lambda^{c_3+2n-1}e^{-(d_3\lambda+\sum_{k=1}^{n}\lambda^2 x_k^{-2\theta})}\left[1-e^{-\lambda^2\tau^{-2\theta}}\right]^{\alpha(n-d)}\prod_{k=1}^{n}\left[1-e^{-\lambda^2 x_k^{-2\theta}}\right]^{\alpha-1}, \tag{21}$$

$$R_1 \propto \alpha^{c_1+n-1}\theta^{c_2+n-1}\lambda^{c_3+2n-1}e^{-(d_1\alpha+d_2\theta+d_3\lambda)}\left[1-e^{-\lambda^2 t^{-2\theta}}\right]\left[1-e^{-\lambda^2\tau^{-2\theta}}\right]^{\alpha(n-d)} \times\prod_{k=1}^{n}x_k^{-2\theta-1}\left[1-e^{-\lambda^2 x_k^{-2\theta}}\right]^{\alpha-1}e^{-\lambda^2 x_k^{-2\theta}}, \tag{22}$$

and

$$H_1 \propto \alpha^{c_1+n-1}\theta^{c_2+n-1}\lambda^{c_3+2n-1}e^{-(d_1\alpha+d_2\theta+d_3\lambda)}\frac{2\alpha\theta\lambda^2 t^{-2\theta-1}}{e^{\lambda^2 t^{-2\theta}}-1}\left[1-e^{-\lambda^2\tau^{-2\theta}}\right]^{\alpha(n-d)} \times\prod_{k=1}^{n}x_k^{-2\theta-1}\left[1-e^{-\lambda^2 x_k^{-2\theta}}\right]^{\alpha-1}e^{-\lambda^2 x_k^{-2\theta}}. \tag{23}$$

Since there are no closed-form formulations for the marginal posterior densities in equations (19)-(23), we shall produce samples for $\alpha,\theta,\lambda$, RF, and HRF using the Metropolis-Hastings (M-H) algorithm with a normal proposal distribution.

The M-H algorithm is a Markov Chain Monte Carlo (MCMC) method used to generate samples from a probability distribution, even when direct sampling is difficult. The algorithm proceeds as follows:

- Initialize:
  - Start with an initial value, which serves as the starting point of the chain.
  - Define the target distribution $l\left(\Psi\middle|\underline{\underline{t}}\right)$ from which we want to sample.
  - Set the number of iterations $I$ and the standard deviation $\sigma_\Psi$ for the normal proposal distribution form Hessian matrix.
- Iterate for $I$ steps:
  - Generate a proposed value from a normal distribution centered at the current value:

$$\Psi \sim \mathcal{N}(\hat{\Psi}, \sigma_\Psi^2).$$

  - Compute the acceptance ratio $R$:

$$R = \min\left(1, \frac{l\left(\Psi^{(i)}\middle|\underline{\underline{t}}\right)}{l\left(\Psi^{(i-1)}\middle|\underline{\underline{t}}\right)}\right).$$

  - Draw a random number $u$ from a uniform distribution $U(0,1)$.
  - If $u \leq R$, accept the proposed value $\Psi$ as the next state: $\Psi^{(i+1)} = \Psi^{(i)}$.
  - Otherwise, retain the current state: $\Psi^{(i+1)} = \Psi^{(i)}$.
- After completing all iterations, the chain of samples represents an approximation of the target distribution.

## 5. Simulation

In this section, we perform a simulation study to evaluate the performance of the proposed methods. We begin by simulating hybrid censored data from the IPB-XD for different values of $n$ and $r$ as follows:

- For $n = 40$, then $r = 28, 35, 40$.
- For $n = 100$, $r = 75, 85, 100$.
- For $n = 150$, $r = 110, 130, 150$.

The various actual parameters and hybrid censored sample time were changed for each scenario as detailed below:

- Table 1: $\alpha = 1.2, \theta = 0.5, \lambda = 0.4$, and $T = 0.25, 0.5, 15$.
- Table 2: $\alpha = 1.2, \theta = 0.5, \lambda = 1.3$, and $T = 2, 5, 150$.
- Table 3: $\alpha = 1.2, \theta = 0.5, \lambda = 3$, and $T = 11, 25, 50$.
- Table 4: $\alpha = 3, \theta = 1.2, \lambda = 1.3$, and $T = 1, 1.3, 4$.

In the simulation study, we compared the ML, MPS, and Bayesian (based on the squared error loss function) estimation methods. Although direct comparison between Bayesian and classical estimation methods (ML and MPS) is typically challenging, we used the ML information to generate Bayesian estimates, enabling comparison between ML and Bayesian estimates. Recent literature also discusses such comparisons between ML and Bayesian estimates, as well as other estimation methods.

The main difference between ML and Bayesian methods lies in the parameters being treated as random variables with prior distributions. We used the gamma distribution as the prior, with shape and scale parameters (hyper-parameters). These hyper-parameters were selected based on ML information and gamma distribution – a process known as elicitation of hyper-parameters, as described by Dey et al. [46].

By setting $\hat{\alpha}, \hat{\theta}$ and $\hat{\lambda}$ equal to the mean and variance of the gamma prior distribution, we can determine their corresponding means and variances. This yields:

$$\frac{1}{I}\sum_{j=1}^{I}\hat{\alpha}^j = c_1 d_1 \quad \& \quad \frac{1}{I-1}\sum_{j=1}^{I}\left(\hat{\alpha}^j - \frac{1}{I}\sum_{j=1}^{I}\hat{\alpha}^j\right)^2 = c_1^2 d_1,$$

$$\frac{1}{I}\sum_{j=1}^{I}\hat{\theta}^j = c_2 d_2 \quad \& \quad \frac{1}{I-1}\sum_{j=1}^{I}\left(\hat{\theta}^j - \frac{1}{I}\sum_{j=1}^{I}\hat{\theta}^j\right)^2 = c_2^2 d_2,$$

$$\frac{1}{I}\sum_{j=1}^{I}\hat{\lambda}^j = c_3 d_3 \quad \& \quad \frac{1}{I-1}\sum_{j=1}^{I}\left(\hat{\lambda}^j - \frac{1}{I}\sum_{j=1}^{I}\hat{\lambda}^j\right)^2 = c_3^2 d_3,$$

where $I$ is the total iteration of the simulation of MCMC method. Now, on solving the above two equations for each hyper-parameter, the estimated hyper-parameters can be written as:

$$c_1 = \frac{\left(\frac{1}{I}\sum_{j=1}^{I}\hat{\alpha}^j\right)^2}{\frac{1}{I-1}\sum_{j=1}^{I}\left(\hat{\alpha}^j - \frac{1}{I}\sum_{j=1}^{I}\hat{\alpha}^j\right)^2} \quad \& \quad d_1 = \frac{\frac{1}{I-1}\sum_{j=1}^{I}\left(\hat{\alpha}^j - \frac{1}{I}\sum_{j=1}^{I}\hat{\alpha}^j\right)^2}{\frac{1}{I}\sum_{j=1}^{I}\hat{\alpha}^j}, \quad (24)$$

$$c_2 = \frac{\left(\frac{1}{I}\sum_{j=1}^{I}\hat{\theta}^j\right)^2}{\frac{1}{I-1}\sum_{j=1}^{I}\left(\hat{\theta}^j - \frac{1}{I}\sum_{j=1}^{I}\hat{\theta}^j\right)^2} \quad \& \quad d_2 = \frac{\frac{1}{I-1}\sum_{j=1}^{I}\left(\hat{\theta}^j - \frac{1}{I}\sum_{j=1}^{I}\hat{\theta}^j\right)^2}{\frac{1}{I}\sum_{j=1}^{I}\hat{\theta}^j}, \quad (25)$$

$$c_3 = \frac{\left(\frac{1}{I}\sum_{j=1}^{I}\hat{\lambda}^j\right)^2}{\frac{1}{I-1}\sum_{j=1}^{I}\left(\hat{\lambda}^j - \frac{1}{I}\sum_{j=1}^{I}\hat{\lambda}^j\right)^2} \quad \& \quad d_3 = \frac{\frac{1}{I-1}\sum_{j=1}^{I}\left(\hat{\lambda}^j - \frac{1}{I}\sum_{j=1}^{I}\hat{\lambda}^j\right)^2}{\frac{1}{I}\sum_{j=1}^{I}\hat{\lambda}^j}. \quad (26)$$

Then, we calculate the ML and MPS estimates of $\alpha, \theta$ and $\lambda$ using the Newton--Raphson (NR) algorithm, and derive Bayesian estimates using the M-H algorithm based on 10,000 Monte Carlo simulations. It's worth mentioning that we used the R programming language to generate the estimates for these calculations. We recommend the use of the 'maxLik' package, which provides classical estimates by applying the NR algorithm for numerical maximization (refer to [47]), and the 'CODA' package, which simulates MCMC to produce Bayesian estimates (see [48]).

The performance of the ML, MPS, and Bayesian estimates was assessed using the mean square error (MSE), the length of confidence intervals, RF, and HRF estimates with $T$ of the censoring scheme. For confidence intervals, the ACIs estimates for ML and MPS were calculated, with their length referred to as L.ACI (see [49, 50]). For Bayesian estimation, the credible confidence interval (L.CCI) was determined. To identify the best estimation method, we selected the smallest MSE values and the shortest confidence interval lengths.

From Tables 1-4, we can conclude the following:

- As the sample size $n$ increases with fixed anther factors as $r$ and $T$, the proposed estimates of $\alpha, \theta$, and $\lambda$ improve in terms of Bias, MSE, and length of intervals.
- The Bias, MSE, and LCI decrease as the sample size of the censored sample $(r)$ increases, indicating improved estimate performance.
- The Bias, MSE, and LCI decrease as the sample size of the censored sample $(T)$ increases, indicating improved estimate performance.
- The decreasing Bias, MSE, and LCI with larger samples clearly demonstrate the accuracy and consistency of the estimators.
- All three estimation methods perform well for the parameters of the IPB-XD.
- The Bayesian estimation method outperforms the other methods in accuracy.
- The LCCI for the Bayesian method is observed to be smaller compared to the traditional LACI of ML and MPS methods, indicating greater precision.

## 6. Application of real data

We employed two real-world datasets to evaluate the effectiveness of the proposed distribution. To do so, we applied various statistical analysis metrics, including the Kolmogorov-Smirnov distance (KOSD) test with its associated p-value (KOSPV),

Table 1. MLE, MPS, and Bayesian estimation methods for parameters and reliability analysis: $\alpha = 1.2, \theta = 0.5, \lambda = 0.4$

| $\alpha=1.2,\theta=0.5,\lambda=0.4$ | | | | MLE | | | MPS | | | Bayesian | | |
|---|---|---|---|---|---|---|---|---|---|---|---|---|
| n | T | r | | Bias | MSE | LACI | Bias | MSE | LACI | Bias | MSE | LCCI |
| 40 | 0.25 | 28 | $\alpha$ | -0.07369 | 0.07840 | 0.86470 | 0.05133 | 0.05128 | 0.46151 | -0.00625 | 0.01662 | 0.48835 |
| | | | $\theta$ | 0.04248 | 0.00690 | 0.31213 | -0.05344 | 0.00575 | 0.32169 | 0.01639 | 0.00505 | 0.26632 |
| | | | $\lambda$ | -0.03959 | 0.00691 | 0.30224 | 0.05585 | 0.00598 | 0.24682 | 0.00221 | 0.00552 | 0.28796 |
| | | | RF | -0.03794 | 0.00550 | 0.28838 | 0.04541 | 0.00539 | 0.26783 | 0.02611 | 0.00543 | 0.29082 |
| | | | HRF | 0.05462 | 0.69777 | 3.16658 | -0.05033 | 0.60504 | 3.29641 | 0.01293 | 0.53319 | 2.80573 |
| | 0.50 | 35 | $\alpha$ | -0.06732 | 0.06145 | 0.84467 | -0.04103 | 0.04842 | 0.44052 | -0.00383 | 0.00978 | 0.39248 |
| | | | $\theta$ | 0.04161 | 0.00500 | 0.26204 | -0.03677 | 0.00410 | 0.27600 | 0.01513 | 0.00306 | 0.21171 |
| | | | $\lambda$ | -0.03530 | 0.00644 | 0.25669 | 0.03482 | 0.00405 | 0.21171 | -0.00183 | 0.00323 | 0.22622 |
| | | | RF | -0.03294 | 0.00264 | 0.19724 | 0.03486 | 0.00272 | 0.18053 | 0.02205 | 0.00252 | 0.19072 |
| | | | HRF | 0.04734 | 0.13552 | 1.38107 | -0.04160 | 0.11358 | 1.44180 | 0.01065 | 0.09637 | 1.21709 |
| | 15 | 40 | $\alpha$ | -0.02243 | 0.05139 | 0.41883 | -0.01826 | 0.01464 | 0.43711 | 0.00055 | 0.00376 | 0.23714 |
| | | | $\theta$ | 0.04043 | 0.00460 | 0.24922 | -0.03182 | 0.00341 | 0.25501 | 0.00780 | 0.00175 | 0.16081 |
| | | | $\lambda$ | -0.03097 | 0.00434 | 0.25403 | 0.02076 | 0.00370 | 0.21129 | -0.00141 | 0.00180 | 0.16333 |
| | | | RF | 0.03263 | 0.00097 | 0.01216 | 0.03255 | 0.00024 | 0.01458 | 0.01970 | 0.00001 | 0.00872 |
| | | | HRF | 0.03857 | 0.00151 | 0.04633 | -0.04097 | 0.00129 | 0.04818 | 0.00833 | 0.00006 | 0.03067 |
| 100 | 0.25 | 75 | $\alpha$ | 0.02550 | 0.05256 | 0.85743 | 0.04404 | 0.04648 | 0.41774 | -0.00297 | 0.01457 | 0.45695 |
| | | | $\theta$ | 0.01833 | 0.00372 | 0.23165 | -0.03755 | 0.00321 | 0.23356 | 0.00876 | 0.00283 | 0.20854 |
| | | | $\lambda$ | -0.01434 | 0.00474 | 0.26627 | 0.05075 | 0.00443 | 0.21764 | 0.00315 | 0.00320 | 0.22466 |
| | | | RF | -0.01192 | 0.00295 | 0.17023 | 0.00545 | 0.00190 | 0.16131 | 0.01063 | 0.00172 | 0.19082 |
| | | | HRF | 0.03078 | 0.25156 | 1.81990 | -0.01723 | 0.20987 | 1.92393 | 0.00236 | 0.20050 | 1.91102 |
| | 0.50 | 85 | $\alpha$ | 0.02513 | 0.05061 | 0.82791 | 0.03636 | 0.04554 | 0.38179 | -0.00211 | 0.00896 | 0.36397 |
| | | | $\theta$ | 0.01008 | 0.00352 | 0.22700 | -0.03585 | 0.00299 | 0.22192 | 0.00300 | 0.00191 | 0.16802 |
| | | | $\lambda$ | -0.00232 | 0.00451 | 0.23747 | 0.03165 | 0.00401 | 0.20214 | 0.00305 | 0.00226 | 0.18714 |
| | | | RF | -0.01096 | 0.00162 | 0.13201 | 0.00480 | 0.00119 | 0.12523 | 0.01023 | 0.00115 | 0.15182 |
| | | | HRF | 0.02956 | 0.06761 | 0.97913 | -0.00713 | 0.06064 | 1.02268 | -0.00236 | 0.06021 | 0.95450 |
| | 15 | 100 | $\alpha$ | 0.01358 | 0.04613 | 0.40810 | 0.01686 | 0.01358 | 0.36924 | -0.00083 | 0.00354 | 0.22531 |
| | | | $\theta$ | 0.00910 | 0.00250 | 0.21688 | -0.01748 | 0.00293 | 0.21372 | 0.00278 | 0.00108 | 0.12186 |
| | | | $\lambda$ | -0.00217 | 0.00348 | 0.20311 | 0.02024 | 0.00306 | 0.20086 | -0.00303 | 0.00118 | 0.12925 |
| | | | RF | 0.00786 | 0.00051 | 0.00877 | 0.00422 | 0.00007 | 0.00900 | 0.00618 | 0.00004 | 0.00720 |
| | | | HRF | 0.02547 | 0.00103 | 0.03877 | -0.00615 | 0.00090 | 0.03964 | 0.00165 | 0.00039 | 0.02365 |
| 150 | 0.25 | 110 | $\alpha$ | 0.01279 | 0.00319 | 0.16415 | 0.02039 | 0.00337 | 0.18306 | -0.00093 | 0.00136 | 0.44039 |
| | | | $\theta$ | 0.01700 | 0.00136 | 0.13659 | -0.01815 | 0.00141 | 0.16086 | 0.00446 | 0.00129 | 0.16514 |
| | | | $\lambda$ | -0.01229 | 0.00133 | 0.13723 | 0.01935 | 0.00165 | 0.13689 | 0.00394 | 0.00122 | 0.17756 |
| | | | RF | -0.01121 | 0.00129 | 0.13594 | -0.00465 | 0.00122 | 0.12887 | 0.00947 | 0.00106 | 0.14795 |
| | | | HRF | 0.03031 | 0.13897 | 1.36433 | -0.00345 | 0.11639 | 1.44141 | -0.00070 | 0.10283 | 1.64679 |
| | 0.50 | 130 | $\alpha$ | 0.01189 | 0.00293 | 0.15982 | 0.02007 | 0.00335 | 0.16212 | 0.00093 | 0.00128 | 0.35449 |
| | | | $\theta$ | 0.00916 | 0.00107 | 0.12246 | -0.01802 | 0.00116 | 0.14503 | 0.00376 | 0.00104 | 0.14675 |
| | | | $\lambda$ | -0.00208 | 0.00109 | 0.12431 | 0.01816 | 0.00137 | 0.12525 | -0.00333 | 0.00106 | 0.15391 |
| | | | RF | -0.01040 | 0.00067 | 0.09591 | -0.00412 | 0.00062 | 0.09020 | 0.00088 | 0.00062 | 0.11787 |
| | | | HRF | 0.02312 | 0.03256 | 0.65245 | 0.00246 | 0.02684 | 0.68875 | 0.00061 | 0.02304 | 0.77724 |
| | 15 | 150 | $\alpha$ | 0.00829 | 0.00284 | 0.13555 | 0.01072 | 0.00300 | 0.15380 | -0.00065 | 0.00123 | 0.23006 |
| | | | $\theta$ | 0.00293 | 0.00104 | 0.10244 | -0.01250 | 0.00105 | 0.14059 | 0.00098 | 0.00090 | 0.11838 |
| | | | $\lambda$ | -0.00208 | 0.00084 | 0.11734 | 0.01720 | 0.00092 | 0.11636 | 0.00304 | 0.00071 | 0.12661 |
| | | | RF | 0.00535 | 0.00000 | 0.00684 | 0.00216 | 0.00004 | 0.00684 | 0.00057 | 0.00000 | 0.00679 |
| | | | HRF | 0.01349 | 0.00004 | 0.02352 | -0.00137 | 0.00035 | 0.02503 | -0.00038 | 0.00003 | 0.02230 |

Cramér-von Mises (CVOM), and Anderson-Darling (AnD) tests. Additionally, we used several criteria, such as the Akaike information criterion (AkInC), and Bayesian information criterion (BInC). The hybrid censored samples have also been checked for two datasets. The IPB-XD distribution was compared with several distributions, including PB-XD, sine-exponentiated Weibull exponential distribution (SEWED) by [51], generalized inverse Weibull distribution (GIWD) by [52], exponentiated sine Weibull distribution (ESWD) by [53], Burr III distribution (BIIID) by [1], inverse power Lindley distribution (IPLD) [15], and generalized inverse power Sujatha distribution (GIPSD) by [54].

### 6.1. Data I

The first dataset, originally from Gacula and Kubala [55], consists of 26 failure time observations for a specific product. This dataset has also been referenced by Elbatal et al. [56]. The recorded failure times are: 24, 24, 26, 26, 32, 32, 33, 33,

Table 2. MLE, MPS, and Bayesian estimation methods for parameters and reliability analysis: $\alpha = 1.2, \theta = 0.5, \lambda = 1.3$

| $\alpha=1.2,\theta=0.5,\lambda=1.3$ | | | | MLE | | | MPS | | | Bayesian | | |
|---|---|---|---|---|---|---|---|---|---|---|---|---|
| n | T | r | | Bias | MSE | LACI | Bias | MSE | LACI | Bias | MSE | LCCI |
| 40 | 2 | 28 | $\alpha$ | -0.21118 | 0.53205 | 3.59440 | 0.15952 | 0.50532 | 2.49979 | -0.00938 | 0.01569 | 0.47279 |
| | | | $\theta$ | 0.48290 | 0.21558 | 1.51635 | 0.16621 | 0.09602 | 1.32711 | 0.01410 | 0.00761 | 0.33650 |
| | | | $\lambda$ | -0.14832 | 0.14738 | 1.37106 | -0.07774 | 0.09648 | 1.10719 | 0.00315 | 0.00972 | 0.37770 |
| | | | RF | 0.00674 | 0.00584 | 0.29521 | 0.02537 | 0.00547 | 0.27257 | 0.02863 | 0.00517 | 0.29175 |
| | | | HRF | -0.02622 | 0.01182 | 0.42028 | -0.09689 | 0.01063 | 0.40196 | 0.01781 | 0.00931 | 0.36562 |
| | 5 | 35 | $\alpha$ | -0.14644 | 0.39102 | 2.38877 | -0.02808 | 0.33477 | 2.10713 | -0.00713 | 0.00870 | 0.36902 |
| | | | $\theta$ | 0.40239 | 0.15573 | 1.30567 | 0.16579 | 0.07518 | 1.13973 | 0.00821 | 0.00437 | 0.26342 |
| | | | $\lambda$ | -0.11607 | 0.10654 | 1.18972 | -0.06813 | 0.07545 | 0.98971 | -0.00249 | 0.00583 | 0.29278 |
| | | | RF | 0.00458 | 0.00352 | 0.22917 | 0.02061 | 0.00359 | 0.21275 | 0.01998 | 0.00306 | 0.20613 |
| | | | HRF | -0.02590 | 0.00255 | 0.19421 | -0.07704 | 0.00213 | 0.17834 | 0.00132 | 0.00122 | 0.13405 |
| | 150 | 40 | $\alpha$ | -0.07445 | 0.30226 | 2.18978 | -0.02723 | 0.26087 | 1.95510 | -0.00253 | 0.00381 | 0.24000 |
| | | | $\theta$ | 0.26778 | 0.09949 | 1.08659 | 0.15205 | 0.05849 | 0.95660 | 0.00742 | 0.00266 | 0.19282 |
| | | | $\lambda$ | -0.06189 | 0.06849 | 1.05246 | -0.06074 | 0.05810 | 0.91797 | -0.00233 | 0.00341 | 0.22099 |
| | | | RF | 0.00438 | 0.00031 | 0.02059 | 0.01881 | 0.00055 | 0.02217 | 0.01690 | 0.00013 | 0.01106 |
| | | | HRF | 0.00815 | 0.00040 | 0.00772 | -0.07075 | 0.00032 | 0.00714 | 0.00126 | 0.00008 | 0.00348 |
| 100 | 2 | 75 | $\alpha$ | -0.06494 | 0.33374 | 2.23143 | 0.14060 | 0.35688 | 2.00271 | -0.00733 | 0.01431 | 0.45800 |
| | | | $\theta$ | 0.16803 | 0.04609 | 0.76109 | -0.00536 | 0.02150 | 0.65895 | 0.01211 | 0.00380 | 0.23522 |
| | | | $\lambda$ | -0.06499 | 0.06011 | 0.95668 | -0.00667 | 0.03880 | 0.74311 | -0.00228 | 0.00492 | 0.26533 |
| | | | RF | 0.00655 | 0.00210 | 0.17743 | 0.00996 | 0.00206 | 0.16962 | -0.00372 | 0.00206 | 0.19528 |
| | | | HRF | -0.01590 | 0.00508 | 0.27556 | -0.03922 | 0.00446 | 0.26311 | 0.01289 | 0.00436 | 0.24838 |
| | 5 | 85 | $\alpha$ | -0.05465 | 0.22219 | 2.13859 | 0.01638 | 0.20810 | 1.57866 | -0.00685 | 0.00809 | 0.36067 |
| | | | $\theta$ | 0.09270 | 0.02619 | 0.60582 | -0.00508 | 0.01324 | 0.49831 | 0.00747 | 0.00207 | 0.17911 |
| | | | $\lambda$ | -0.04498 | 0.03809 | 0.83891 | -0.00612 | 0.02709 | 0.63192 | -0.00221 | 0.00398 | 0.25000 |
| | | | RF | 0.00448 | 0.00149 | 0.14851 | 0.00829 | 0.00141 | 0.13838 | 0.00358 | 0.00140 | 0.14733 |
| | | | HRF | -0.00829 | 0.00116 | 0.13166 | -0.02752 | 0.00096 | 0.12143 | 0.00073 | 0.00056 | 0.09197 |
| | 150 | 100 | $\alpha$ | -0.01015 | 0.17780 | 1.91150 | 0.01618 | 0.16370 | 1.53668 | -0.00028 | 0.00359 | 0.23459 |
| | | | $\theta$ | 0.07037 | 0.02147 | 0.53974 | 0.00424 | 0.01304 | 0.48951 | 0.00524 | 0.00154 | 0.14791 |
| | | | $\lambda$ | -0.02701 | 0.02810 | 0.75459 | -0.00597 | 0.02350 | 0.61316 | 0.00161 | 0.00246 | 0.19892 |
| | | | RF | 0.00416 | 0.00012 | 0.01335 | 0.00733 | 0.00015 | 0.01311 | 0.00327 | 0.00006 | 0.00859 |
| | | | HRF | 0.00801 | 0.00019 | 0.00538 | -0.02338 | 0.00016 | 0.00519 | 0.00126 | 0.00005 | 0.00253 |
| 150 | 2 | 110 | $\alpha$ | -0.04128 | 0.26446 | 1.17686 | 0.09929 | 0.10454 | 0.88303 | -0.00100 | 0.01350 | 0.44689 |
| | | | $\theta$ | -0.08179 | 0.03675 | 0.70241 | -0.00508 | 0.00396 | 0.20189 | 0.00990 | 0.00248 | 0.19580 |
| | | | $\lambda$ | -0.02759 | 0.03259 | 0.88833 | 0.00516 | 0.00877 | 0.31429 | 0.00057 | 0.00385 | 0.24276 |
| | | | RF | 0.00056 | 0.00012 | 0.00516 | 0.00934 | 0.00015 | 0.00413 | 0.00077 | 0.00004 | 0.00171 |
| | | | HRF | 0.01451 | 0.00360 | 0.25733 | -0.02700 | 0.00255 | 0.22117 | 0.00692 | 0.00247 | 0.19559 |
| | 5 | 130 | $\alpha$ | -0.02072 | 0.16054 | 1.06547 | 0.01468 | 0.09169 | 0.80424 | -0.00094 | 0.00804 | 0.36044 |
| | | | $\theta$ | 0.06629 | 0.01481 | 0.44289 | -0.00457 | 0.00292 | 0.19413 | 0.00611 | 0.00173 | 0.15419 |
| | | | $\lambda$ | -0.02489 | 0.02354 | 0.67138 | -0.00411 | 0.00718 | 0.30511 | -0.00042 | 0.00303 | 0.20798 |
| | | | RF | -0.00051 | 0.00012 | 0.00402 | 0.00813 | 0.00013 | 0.00411 | 0.00034 | 0.00003 | 0.00125 |
| | | | HRF | -0.00340 | 0.00078 | 0.10822 | -0.01028 | 0.00069 | 0.10286 | 0.00045 | 0.00040 | 0.07823 |
| | 150 | 150 | $\alpha$ | -0.00958 | 0.12084 | 1.05704 | 0.01348 | 0.07925 | 0.80125 | -0.00021 | 0.00340 | 0.23060 |
| | | | $\theta$ | 0.03852 | 0.01126 | 0.40512 | 0.00299 | 0.00184 | 0.18375 | 0.00429 | 0.00133 | 0.14339 |
| | | | $\lambda$ | -0.01387 | 0.01524 | 0.57000 | -0.00312 | 0.00613 | 0.19454 | -0.00041 | 0.00198 | 0.17197 |
| | | | RF | 0.00277 | 0.00008 | 0.01075 | 0.00625 | 0.00009 | 0.01044 | 0.00180 | 0.00004 | 0.00770 |
| | | | HRF | 0.00303 | 0.00013 | 0.00438 | -0.01892 | 0.00011 | 0.00420 | 0.00094 | 0.00004 | 0.00231 |

33, 35, 41, 42, 43, 47, 48, 48, 48, 50, 52, 54, 55, 57, 57, 57, 57, and 61. The first dataset consists of 26 discrete lifetime observations, with a total sum of 1115 and a mean value of 42.88. The standard deviation is 11.84, indicating moderate dispersion around the mean. The median is 45, while the mode is 57, suggesting a slight concentration toward higher values. The coefficient of variation (CV) is 0.276, reflecting relative variability. The skewness is –0.175, indicating a slight leftward asymmetry, and the kurtosis is –1.322, suggesting a relatively flat distribution compared to the normal distribution. Table 5 provides the ML estimate (MLE) with standard errors (StEr), along with various metrics for evaluating the failure time data. The table compares our model against several other distributions, such as PB-XD, SEWED, APIWD, GIWD, ESWD, BIIID, IPLD, and GIPSD. The findings indicate that the IPB-XD achieved the smallest values for the metrics AKInC, BInC, KOSD, CVOM, and AnD, while the highest values were noted for KOSPV. These results suggest that the IPB-XD was the most suitable model for fitting the failure time data. Figure 6

Table 3. MLE, MPS, and Bayesian estimation methods for parameters and reliability analysis: $\alpha = 1.2, \theta = 0.5, \lambda = 3$

| $\alpha=1.2,\theta=0.5,\lambda=3$ | | | | MLE | | | MPS | | | Bayesian | | |
|---|---|---|---|---|---|---|---|---|---|---|---|---|
| n | T | r | | Bias | MSE | LACI | Bias | MSE | LACI | Bias | MSE | LCCI |
| 40 | 11 | 28 | $\alpha$ | -0.05931 | 0.22180 | 1.62847 | 0.03833 | 0.18747 | 1.65008 | -0.00696 | 0.01718 | 0.51051 |
| | | | $\theta$ | 0.13126 | 0.02169 | 0.52660 | -0.04095 | 0.01355 | 0.52230 | 0.00724 | 0.00257 | 0.18642 |
| | | | $\lambda$ | 0.07061 | 0.36029 | 2.18186 | -0.04351 | 0.22841 | 2.12401 | -0.00388 | 0.01684 | 0.50342 |
| | | | RF | -0.00956 | 0.00563 | 0.29061 | 0.01819 | 0.00544 | 0.27155 | 0.00162 | 0.00446 | 0.30826 |
| | | | HRF | 0.06183 | 0.00342 | 0.07160 | -0.07418 | 0.00309 | 0.07153 | 0.00421 | 0.00087 | 0.05133 |
| | 25 | 35 | $\alpha$ | -0.05814 | 0.20544 | 1.60733 | -0.01912 | 0.18641 | 1.62659 | -0.00524 | 0.00977 | 0.37587 |
| | | | $\theta$ | 0.12223 | 0.02027 | 0.49599 | 0.01717 | 0.01357 | 0.50436 | 0.00586 | 0.00188 | 0.16657 |
| | | | $\lambda$ | 0.06165 | 0.20111 | 1.57852 | -0.03051 | 0.14397 | 1.70291 | -0.00288 | 0.00885 | 0.36160 |
| | | | RF | 0.00840 | 0.00367 | 0.23334 | 0.01666 | 0.00358 | 0.21560 | 0.00148 | 0.00307 | 0.23121 |
| | | | HRF | -0.04406 | 0.00318 | 0.03536 | -0.07327 | 0.00253 | 0.03381 | 0.00303 | 0.00029 | 0.02095 |
| | 50 | 40 | $\alpha$ | 0.03681 | 0.20118 | 1.57771 | -0.00827 | 0.16200 | 1.47942 | 0.00504 | 0.00393 | 0.23849 |
| | | | $\theta$ | 0.07165 | 0.01583 | 0.46818 | 0.01620 | 0.01047 | 0.49717 | 0.00331 | 0.00132 | 0.14246 |
| | | | $\lambda$ | 0.05551 | 0.17176 | 1.46640 | -0.02510 | 0.12722 | 1.59149 | 0.00050 | 0.00370 | 0.23943 |
| | | | RF | 0.00821 | 0.00278 | 0.20228 | 0.01578 | 0.00057 | 0.02277 | 0.00141 | 0.00001 | 0.01113 |
| | | | HRF | 0.04071 | 0.00142 | 0.01436 | -0.05946 | 0.00116 | 0.01427 | 0.00289 | 0.00018 | 0.00053 |
| 100 | 11 | 75 | $\alpha$ | -0.04118 | 0.10827 | 1.22292 | -0.03063 | 0.06684 | 0.96835 | -0.00662 | 0.01581 | 0.49135 |
| | | | $\theta$ | 0.10890 | 0.01729 | 0.46323 | 0.01074 | 0.00710 | 0.37698 | 0.00368 | 0.00142 | 0.14541 |
| | | | $\lambda$ | 0.03328 | 0.08918 | 1.08714 | -0.02444 | 0.06842 | 1.14696 | -0.00074 | 0.01514 | 0.47506 |
| | | | RF | 0.00604 | 0.00211 | 0.17776 | 0.01701 | 0.00213 | 0.17004 | 0.00131 | 0.00205 | 0.18777 |
| | | | HRF | -0.03068 | 0.00130 | 0.04345 | -0.06782 | 0.00125 | 0.04217 | -0.00415 | 0.00077 | 0.03403 |
| | 25 | 85 | $\alpha$ | -0.02804 | 0.03679 | 0.78401 | -0.01157 | 0.02867 | 0.67479 | -0.00160 | 0.00878 | 0.36310 |
| | | | $\theta$ | 0.02920 | 0.00399 | 0.23966 | -0.00916 | 0.00286 | 0.22701 | 0.00250 | 0.00094 | 0.12253 |
| | | | $\lambda$ | 0.01539 | 0.04205 | 0.77251 | -0.02269 | 0.04133 | 0.87942 | -0.00038 | 0.00884 | 0.36330 |
| | | | RF | 0.00579 | 0.00129 | 0.13881 | 0.01538 | 0.00138 | 0.13251 | 0.00124 | 0.00115 | 0.14696 |
| | | | HRF | -0.00886 | 0.00023 | 0.01870 | -0.04044 | 0.00021 | 0.01893 | -0.00026 | 0.00013 | 0.01421 |
| | 50 | 100 | $\alpha$ | 0.02016 | 0.03611 | 0.75091 | -0.00721 | 0.02362 | 0.60774 | -0.00049 | 0.00368 | 0.23148 |
| | | | $\theta$ | 0.02011 | 0.00259 | 0.19328 | -0.00812 | 0.00278 | 0.21479 | 0.00231 | 0.00069 | 0.10193 |
| | | | $\lambda$ | 0.01481 | 0.03686 | 0.71521 | -0.01688 | 0.03764 | 0.83091 | -0.00012 | 0.00349 | 0.22601 |
| | | | RF | 0.00374 | 0.00071 | 0.09104 | 0.01427 | 0.00011 | 0.01078 | 0.00114 | 0.00004 | 0.00736 |
| | | | HRF | 0.00715 | 0.00019 | 0.00739 | -0.03202 | 0.00034 | 0.00077 | 0.00020 | 0.00013 | 0.00037 |
| 150 | 11 | 110 | $\alpha$ | 0.04066 | 0.09102 | 0.39303 | 0.01367 | 0.01060 | 0.37722 | -0.00618 | 0.01004 | 0.41967 |
| | | | $\theta$ | 0.05216 | 0.01151 | 0.13142 | -0.00932 | 0.00148 | 0.15770 | 0.00265 | 0.00118 | 0.13663 |
| | | | $\lambda$ | 0.00683 | 0.03999 | 0.77012 | -0.02249 | 0.04416 | 0.85886 | -0.00062 | 0.01344 | 0.44253 |
| | | | RF | -0.00189 | 0.00015 | 0.00061 | 0.00755 | 0.00031 | 0.14338 | -0.00121 | 0.00011 | 0.15649 |
| | | | HRF | 0.00477 | 0.00007 | 0.00632 | -0.03060 | 0.00027 | 0.00063 | 0.00012 | 0.00002 | 0.00028 |
| | 25 | 130 | $\alpha$ | 0.02401 | 0.01070 | 0.27015 | 0.00932 | 0.01027 | 0.30193 | -0.00157 | 0.00692 | 0.35697 |
| | | | $\theta$ | 0.02824 | 0.00278 | 0.12041 | -0.00814 | 0.00120 | 0.14620 | 0.00207 | 0.00076 | 0.10929 |
| | | | $\lambda$ | 0.00610 | 0.03827 | 0.74969 | -0.02127 | 0.03744 | 0.80063 | -0.00030 | 0.00850 | 0.35597 |
| | | | RF | -0.00172 | 0.00013 | 0.00051 | 0.00580 | 0.00018 | 0.10589 | -0.00102 | 0.00009 | 0.11357 |
| | | | HRF | 0.00281 | 0.00002 | 0.00516 | -0.00462 | 0.00016 | 0.00042 | 0.00009 | 0.00001 | 0.00011 |
| | 50 | 150 | $\alpha$ | 0.01519 | 0.00927 | 0.17023 | 0.00625 | 0.00932 | 0.29610 | -0.00042 | 0.00356 | 0.23235 |
| | | | $\theta$ | 0.01543 | 0.00244 | 0.11825 | -0.00711 | 0.00102 | 0.12059 | 0.00201 | 0.00050 | 0.08707 |
| | | | $\lambda$ | 0.00515 | 0.03049 | 0.68397 | -0.01180 | 0.03376 | 0.78177 | -0.00010 | 0.00347 | 0.22272 |
| | | | RF | 0.00130 | 0.00001 | 0.00050 | 0.00511 | 0.00001 | 0.00961 | 0.00100 | 0.00000 | 0.00623 |
| | | | HRF | 0.00613 | 0.00001 | 0.00072 | -0.01310 | 0.00033 | 0.00074 | 0.00013 | 0.00001 | 0.00032 |

supports these conclusions, which give the estimated PDF, CDF, PP-plot and QQ-plot for the IPB-XD applied to the dataset I.

Table 6 compares three estimation methods: ML, MPS, and Bayesian for the parameters ($\alpha$, $\theta$, and $\lambda$) of the IPB-XD model based on hybrid-censored samples from Data I. The table presents the parameter estimates, StEr, confidence intervals (Lower and Upper bounds), and reliability measures (RF and HRF) for a different censored time $(T)$. It shows how the estimates vary across methods and sample configurations. Notably, the ML method tends to provide higher estimates for $\alpha$, while Bayesian estimation yields smaller StEr for some cases, indicating potentially greater precision. The reliability measures (RF and HRF) suggest that certain methods may perform better under different sample sizes and censoring scenarios.

Figure 7 illustrates MCMC plots for Data I under two scenarios: $T = 18$, $r = 45$, and $T = 18$, $r = 52$. In both cases, the trace plots for each parameter ($\alpha$, $\theta$, and $\lambda$) display consistent oscillations, indicating effective chain mixing and convergence during the iterations. The autocorrelation plots for each parameter decrease rapidly,

Table 4. MLE, MPS, and Bayesian estimation methods for parameters and reliability analysis: $\alpha = 3, \theta = 1.2, \lambda = 1.3$

| $\alpha=3,\theta=1.2,\lambda=1.3$ | | | | MLE | | | MPS | | | Bayesian | | |
|---|---|---|---|---|---|---|---|---|---|---|---|---|
| n | T | r | | Bias | MSE | LACI | Bias | MSE | LACI | Bias | MSE | LCCI |
| 40 | 1 | 28 | $\alpha$ | -0.05673 | 0.59749 | 2.93218 | 0.01687 | 0.41268 | 2.30784 | -0.00735 | 0.01893 | 0.53409 |
| | | | $\theta$ | 0.10058 | 0.11559 | 1.24064 | -0.05395 | 0.06347 | 1.12833 | -0.00421 | 0.01464 | 0.48050 |
| | | | $\lambda$ | -0.03817 | 0.02567 | 0.65867 | -0.03476 | 0.01345 | 0.45829 | -0.00166 | 0.00581 | 0.28988 |
| | | | RF | -0.01388 | 0.00554 | 0.28718 | 0.00907 | 0.00528 | 0.26820 | -0.00256 | 0.00527 | 0.27697 |
| | | | HRF | 0.05155 | 0.61971 | 3.00644 | -0.07152 | 0.54499 | 3.09073 | 0.00312 | 0.25805 | 1.92744 |
| | 1.3 | 35 | $\alpha$ | -0.04102 | 0.49076 | 2.39768 | -0.01540 | 0.40677 | 1.97697 | -0.00111 | 0.00971 | 0.39096 |
| | | | $\theta$ | 0.09138 | 0.11399 | 1.13134 | 0.01766 | 0.06040 | 1.02173 | -0.00165 | 0.00802 | 0.35313 |
| | | | $\lambda$ | -0.02457 | 0.02394 | 0.60875 | -0.03179 | 0.01252 | 0.44628 | 0.00153 | 0.00462 | 0.26238 |
| | | | RF | -0.01260 | 0.00294 | 0.20985 | 0.00860 | 0.00318 | 0.19694 | 0.00207 | 0.00217 | 0.17829 |
| | | | HRF | 0.01326 | 0.51108 | 2.76920 | -0.06594 | 0.46798 | 2.77004 | -0.00251 | 0.16392 | 1.57863 |
| | 4 | 40 | $\alpha$ | -0.04016 | 0.48725 | 2.25828 | -0.01476 | 0.38861 | 1.61309 | -0.00084 | 0.00411 | 0.25099 |
| | | | $\theta$ | 0.08125 | 0.10369 | 1.03228 | 0.01443 | 0.05861 | 0.93144 | -0.00158 | 0.00367 | 0.23263 |
| | | | $\lambda$ | -0.02154 | 0.02345 | 0.60098 | -0.03055 | 0.01133 | 0.38384 | 0.00146 | 0.00264 | 0.20101 |
| | | | RF | 0.01092 | 0.00241 | 0.09234 | 0.00849 | 0.00131 | 0.00347 | 0.00192 | 0.00120 | 0.00051 |
| | | | HRF | -0.00265 | 0.13926 | 1.44585 | -0.06424 | 0.14131 | 1.47955 | -0.00203 | 0.01111 | 0.40910 |
| 100 | 1 | 75 | $\alpha$ | -0.01820 | 0.25414 | 1.87570 | 0.01498 | 0.25601 | 1.79798 | 0.00112 | 0.01729 | 0.49309 |
| | | | $\theta$ | 0.02740 | 0.02918 | 0.65208 | -0.04005 | 0.02461 | 0.65868 | -0.00374 | 0.01120 | 0.41472 |
| | | | $\lambda$ | -0.01074 | 0.00684 | 0.38876 | 0.01045 | 0.00527 | 0.29366 | 0.00128 | 0.00271 | 0.20916 |
| | | | RF | -0.00671 | 0.00211 | 0.17773 | 0.00462 | 0.00210 | 0.17089 | 0.00246 | 0.00203 | 0.18609 |
| | | | HRF | 0.01903 | 0.21479 | 1.78143 | -0.04130 | 0.21741 | 1.91845 | -0.00306 | 0.15835 | 1.53493 |
| | 1.3 | 85 | $\alpha$ | -0.01725 | 0.23662 | 1.81208 | 0.01361 | 0.23607 | 1.60537 | -0.00107 | 0.00928 | 0.38375 |
| | | | $\theta$ | 0.02471 | 0.02423 | 0.60772 | -0.01760 | 0.02300 | 0.74522 | 0.00123 | 0.00623 | 0.30573 |
| | | | $\lambda$ | -0.01024 | 0.00617 | 0.30553 | -0.00630 | 0.00510 | 0.19486 | -0.00102 | 0.00213 | 0.18124 |
| | | | RF | -0.00590 | 0.00128 | 0.13900 | 0.00373 | 0.00137 | 0.13401 | 0.00187 | 0.00114 | 0.13011 |
| | | | HRF | 0.00435 | 0.20189 | 1.68085 | -0.02988 | 0.21944 | 1.88109 | 0.00075 | 0.11681 | 1.30890 |
| | 4 | 100 | $\alpha$ | 0.01030 | 0.21418 | 1.04228 | 0.01211 | 0.20812 | 1.50721 | 0.00019 | 0.00363 | 0.23577 |
| | | | $\theta$ | 0.02352 | 0.02035 | 0.58716 | -0.01069 | 0.02093 | 0.74711 | 0.00112 | 0.00314 | 0.22210 |
| | | | $\lambda$ | -0.00789 | 0.00515 | 0.30507 | -0.00500 | 0.00495 | 0.18350 | 0.00055 | 0.00169 | 0.16204 |
| | | | RF | 0.00349 | 0.00077 | 0.00911 | 0.00061 | 0.00018 | 0.00333 | 0.00130 | 0.00018 | 0.00043 |
| | | | HRF | 0.00202 | 0.08966 | 1.14911 | -0.02882 | 0.08517 | 1.19518 | 0.00061 | 0.00927 | 0.36662 |
| 150 | 1 | 110 | $\alpha$ | -0.01542 | 0.23439 | 1.73263 | -0.01488 | 0.23066 | 1.60470 | 0.00023 | 0.01711 | 0.45119 |
| | | | $\theta$ | 0.02516 | 0.02033 | 0.62706 | -0.00928 | 0.02061 | 0.62758 | 0.00349 | 0.01109 | 0.38420 |
| | | | $\lambda$ | -0.01003 | 0.00510 | 0.32044 | -0.00972 | 0.00507 | 0.23528 | 0.00108 | 0.00189 | 0.15983 |
| | | | RF | -0.00316 | 0.00138 | 0.14447 | 0.00410 | 0.00134 | 0.13751 | 0.00204 | 0.00126 | 0.15172 |
| | | | HRF | 0.01017 | 0.15136 | 1.50420 | -0.03216 | 0.13787 | 1.51973 | 0.00237 | 0.13843 | 1.43065 |
| | 1.3 | 130 | $\alpha$ | -0.01538 | 0.05130 | 0.98182 | 0.00511 | 0.04635 | 0.81588 | -0.00010 | 0.00910 | 0.36993 |
| | | | $\theta$ | 0.01132 | 0.00734 | 0.32762 | -0.00233 | 0.00747 | 0.35832 | -0.00093 | 0.00547 | 0.28307 |
| | | | $\lambda$ | -0.00523 | 0.00189 | 0.18773 | 0.00104 | 0.00176 | 0.15699 | 0.00100 | 0.00149 | 0.15299 |
| | | | RF | 0.00210 | 0.00083 | 0.11123 | 0.00341 | 0.00086 | 0.10528 | 0.00172 | 0.00082 | 0.11762 |
| | | | HRF | 0.00123 | 0.11386 | 1.30555 | -0.02934 | 0.11319 | 1.35938 | -0.00061 | 0.10036 | 1.20257 |
| | 4 | 150 | $\alpha$ | -0.00850 | 0.04858 | 0.81554 | -0.00481 | 0.03623 | 0.71357 | 0.00010 | 0.00319 | 0.22412 |
| | | | $\theta$ | 0.01062 | 0.00722 | 0.31365 | -0.00210 | 0.00746 | 0.32625 | 0.00005 | 0.00308 | 0.20946 |
| | | | $\lambda$ | -0.00430 | 0.00159 | 0.17202 | -0.00101 | 0.00155 | 0.14999 | -0.00045 | 0.00136 | 0.14419 |
| | | | RF | 0.00107 | 0.00008 | 0.00586 | 0.00045 | 0.00004 | 0.00066 | 0.00126 | 0.00001 | 0.00391 |
| | | | HRF | 0.00092 | 0.02169 | 0.57035 | -0.02645 | 0.02193 | 0.60631 | 0.00006 | 0.00880 | 0.35971 |

reflecting minimal autocorrelation between successive samples, which is favorable for parameter estimation accuracy. The posterior density plots exhibit well-defined peaks, indicating the presence of reliable parameter estimates. In the second scenario ($r = 52$), the posterior distributions tend to be slightly broader compared to $r = 45$, suggesting increased variability and lower precision in the parameter estimates due to the higher censoring level. Overall, the plots effectively convey the convergence and mixing quality of the MCMC chains under different censoring conditions.

## 6.2. Data II

The dataset focuses on daily rainfall patterns across Peninsular Malaysia from 1975 to 2004, examining the influence of the southwest and northeast monsoons. These monsoons significantly affect the region's climate, causing distinct seasonal variations in rainfall. The data, which include rainfall intensity measurements at different stations, helps identify spatial and temporal trends over the 30-year period,

Table 5. MLE for IPB-XD and alternative models for Data I

| | | $\alpha$ | $\theta$ | $\lambda$ | $\delta$ | AkInC | BInC | KOSD | KOSPV | CVOM | AnD |
|---|---|---|---|---|---|---|---|---|---|---|---|
| IPB-XD | Estimates | 7934.2758 | 0.2257 | 7.1312 | | 206.8628 | 210.6371 | 0.1490 | 0.6109 | 0.1104 | 0.7088 |
| | StEr | 17059.23 | 0.0613 | 1.0842 | | | | | | | |
| PB-XD | Estimates | 0.8900 | 0.0001 | 2.2935 | | 206.9624 | 210.8367 | 0.1523 | 0.5823 | 0.1197 | 0.7264 |
| | StEr | 0.1537 | 0.0001 | 0.6156 | | | | | | | |
| SEWED | Estimates | 1.6750 | 0.0647 | 0.0347 | 1.0561 | 209.1988 | 214.2312 | 0.1590 | 0.5266 | 0.1295 | 0.7366 |
| | StEr | 2.0660 | 0.0215 | 0.1212 | 0.3151 | | | | | | |
| GIWD | Estimates | 15.4371 | 16.9912 | 3.4156 | | 214.4336 | 215.5245 | 0.1845 | 0.3388 | 0.2019 | 1.2680 |
| | StEr | 3.5156 | 5.0217 | 0.4999 | | | | | | | |
| ESWD | Estimates | 12.9867 | 1.2002 | 0.0182 | | 209.5333 | 213.3076 | 0.1722 | 0.4236 | 0.1447 | 0.9041 |
| | StEr | 8.0697 | 0.1794 | 0.0149 | | | | | | | |
| BIIID | Estimates | 1.4782 | 184.4718 | | | 235.0138 | 237.5300 | 0.3449 | 0.0041 | 0.1647 | 1.0299 |
| | StEr | 0.1279 | 79.0043 | | | | | | | | |
| IPLD | Estimates | 3.4147 | 194391.9 | | | 212.4336 | 214.9498 | 0.1844 | 0.3397 | 0.2018 | 1.2679 |
| | StEr | 0.0521 | 151.1652 | | | | | | | | |
| GIPSD | Estimates | 2.0823 | 0.0073 | 80009261 | | 240.5387 | 244.3130 | 0.2603 | 0.0591 | 0.1753 | 1.0977 |
| | StEr | 0.2002 | 0.0017 | 1677.2 | | | | | | | |

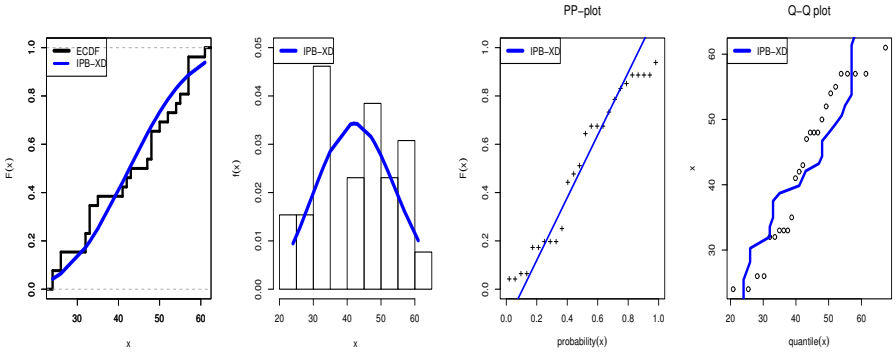


Fig. 6. Plots of Data I and IPB-XD

see [57]. This study uses indices such as total daily rainfall and rainfall frequency to analyze changes and trends. For example, values like 1.47, 1.63, and up to 2.29 represent varying rainfall intensities at different times, showing both regular rainfall events and extreme occurrences. The trends can provide insights into how rainfall patterns are shifting, possibly due to climate change, and inform water resource management and agricultural planning in the region. The data are as follows: 1.47, 1.63, 1.63, 4.94, 5.32, 5.97, 1.76, 1.87, 1.88, 5.38, 5.48, 5.42, 1.92, 2.02, 2.25, 2.27, 2.29, 2.45, 2.59, 3.17, 3.56, 3.78, 3.90, 4.23, 4.76, 6.17, 2.53, 2.74, 3.08, 3.10, 3.12, 3.16, 3.24, 3.27, 3.73, 4.05, 4.22, 4.45, 4.57, 4.88, 4.98, 5.05, 5.14, 5.30, 5.56, 6.20, 6.24, 6.45, 6.51, 6.54. The second dataset comprises 50 continuous observations, with a total sum of 196.22 and a mean of 3.92. The standard deviation is 1.55, and the median is 3.84, close to the mean, indicating symmetry. The mode is 1.63. The coefficient of variation is higher at 0.394, showing greater relative variability than the first dataset. The skewness is 0.081, indicating near symmetry, and the kurtosis is –1.241, also pointing to a flatter distribution than the normal curve.

Table 7 presents the MLE for parameters of the IPB-XD and various alternative models applied to Data II. The models compared include IPB-XD, PB-XD, SEWED, APIWD, GIWD, BIIID, IPLD, and GIPSD. The table lists the parameter estimates

Table 6. ML, MPS, and Bayesian estimation methods for parameters of IPB-XD based on hybrid censored samples: Data I

| $T$ | $r$ | | | Estimates | StEr | Lower | Upper | RF | HRF |
|---|---|---|---|---|---|---|---|---|---|
| 18 | 45 | ML | $\alpha$ | 7933.86655 | 1676.92290 | 4647.09766 | 11220.63543 | 0.48120 | 0.05449 |
| | | | $\theta$ | 0.18038 | 0.00416 | 0.17223 | 0.18853 | | |
| | | | $\lambda$ | 6.05699 | 0.03791 | 5.98269 | 6.13128 | | |
| | | MPS | $\alpha$ | 7934.07740 | 3.81988 | 7926.59043 | 7941.56438 | 0.49910 | 0.04584 |
| | | | $\theta$ | 0.15886 | 0.00186 | 0.15522 | 0.16250 | | |
| | | | $\lambda$ | 5.59588 | 0.03377 | 5.52969 | 5.66207 | | |
| | | Bayesian | $\alpha$ | 7916.05713 | 1685.37308 | 4586.58902 | 11099.01894 | 0.42194 | 0.07897 |
| | | | $\theta$ | 0.22566 | 0.00042 | 0.22483 | 0.22645 | | |
| | | | $\lambda$ | 7.13112 | 0.03794 | 7.05391 | 7.20271 | | |
| | 52 | ML | $\alpha$ | 7932.15819 | 494.04091 | 6963.83800 | 8900.47837 | 0.29632 | 0.07592 |
| | | | $\theta$ | 0.18476 | 0.00167 | 0.18148 | 0.18804 | | |
| | | | $\lambda$ | 6.14989 | 0.02818 | 6.09465 | 6.20513 | | |
| | | MPS | $\alpha$ | 7934.71496 | 3.06767 | 7928.70232 | 7940.72760 | 0.31814 | 0.06515 |
| | | | $\theta$ | 0.16724 | 0.00136 | 0.16457 | 0.16991 | | |
| | | | $\lambda$ | 5.75834 | 0.02488 | 5.70958 | 5.80710 | | |
| | | Bayesian | $\alpha$ | 7929.40048 | 496.16220 | 6948.00852 | 8866.64581 | 0.21470 | 0.11415 |
| | | | $\theta$ | 0.22566 | 0.00017 | 0.22533 | 0.22598 | | |
| | | | $\lambda$ | 7.13112 | 0.02820 | 7.07373 | 7.18436 | | |

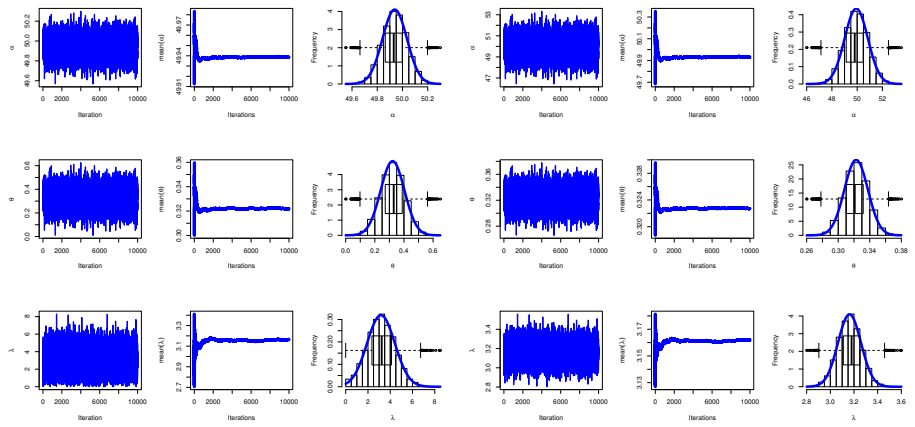

Fig. 7. MCMC plots of Data I

along with their StEr, providing a measure of precision for each estimate. The table also features model comparison criteria, including AkInC, BInC, KOSD, KOSPV, CVOM, and AnD. The results suggest variations in the fit quality across models, with lower AkInC and BInC values generally indicating better model fit. The IPB-XD model exhibits competitive fit measures compared to other models, particularly with relatively low KOSD and CVOM values, suggesting it performs well for Data II. However, some models show lower goodness-of-fit statistics in specific criteria, indicating that the choice of the best model may depend on the criteria prioritized for evaluation. Figure 8 supports these conclusions, which give the estimated PDF, CDF, PP-plot and QQ-plot for the IPB-XD applied to the Dataset II.

Table 8 compares three estimation methods: ML, MPS, and Bayesian with non-informative prior-for the parameters ($\alpha$, $\theta$, and $\lambda$) of the IPB-XD model based on hybrid-censored samples from Data II. The table provides parameter estimates, StEr, and confidence intervals (Lower and Upper bounds) for different levels of censoring $(r)$ and censored time $(T)$. Additionally, it includes reliability measures (RF and

Table 7. MLE for IPB-XD and alternative models for Data II

| | | $\alpha$ | $\theta$ | $\lambda$ | $\delta$ | AkInC | BInC | KOSD | KOSPV | CVOM | AnD |
|---|---|---|---|---|---|---|---|---|---|---|---|
| IPB-XD | Estimates | 12921.84 | 0.1430 | 3.7944 | | 188.5030 | 194.2391 | 0.1064 | 0.6237 | 0.1049 | 0.7077 |
| | StEr | 12.8475 | 0.0206 | 0.1503 | | | | | | | |
| PB-XD | Estimates | 0.2708 | 0.0015 | 3.6714 | | 188.6632 | 194.3993 | 0.1248 | 0.4176 | 0.1094 | 0.7166 |
| | StEr | 0.0372 | 0.0005 | 0.8516 | | | | | | | |
| SEWED | Estimates | 0.0915 | 18.2669 | 2.0184 | 0.0978 | 188.7146 | 195.7943 | 0.1178 | 0.4913 | 0.1098 | 0.7270 |
| | StEr | 0.0109 | 0.0034 | 0.0024 | 0.0028 | | | | | | |
| GIWD | Estimates | 2.8476 | 1.0245 | 2.3191 | | 201.7688 | 202.2905 | 0.1384 | 0.2936 | 0.2721 | 1.6870 |
| | StEr | 150.266 | 125.371 | 0.2441 | | | | | | | |
| BIIID | Estimates | 2.4123 | 13.6165 | | | 199.0877 | 202.9117 | 0.1358 | 0.3148 | 0.2586 | 1.6146 |
| | StEr | 0.2361 | 3.2301 | | | | | | | | |
| IPLD | Estimates | 2.3138 | 12.4111 | | | 199.8275 | 203.6516 | 0.1470 | 0.2302 | 0.2697 | 1.6739 |
| | StEr | 0.2459 | 2.9387 | | | | | | | | |
| GIPSD | Estimates | 2.1197 | 0.0138 | 6292575 | | 208.4476 | 214.1836 | 0.1497 | 0.2123 | 0.2877 | 1.7702 |
| | StEr | 0.2516 | 0.0013 | 315.0265 | | | | | | | |

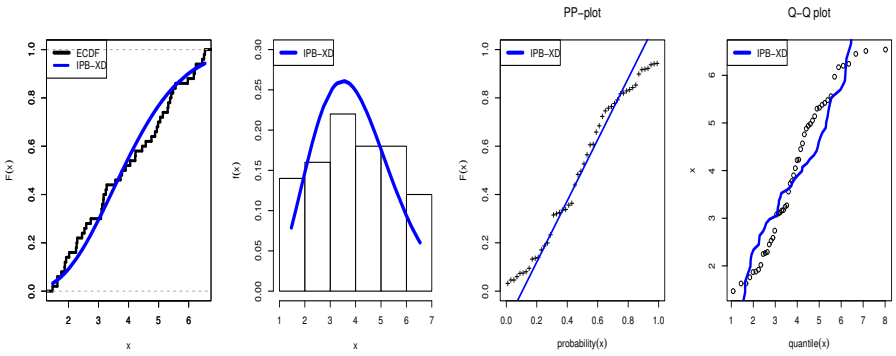


Fig. 8. Plots of Data II and IPB-XD

HRF) for each estimation method under different configurations. The table shows variations in parameter estimates and precision across methods, with Bayesian estimation often producing smaller standard errors, suggesting higher estimation accuracy in some cases. The MPS method typically shows intermediate performance, while the ML method offers wider confidence intervals. The reliability measures (RF and HRF) indicate differences in the performance of the estimation methods under varying censoring levels, helping to identify the most suitable approach for analyzing censored data.

Figure 9 presents MCMC plots for the parameters of Data II under two scenarios: $r = 40$, $T = 3.8$, and $r = 40$, $T = 4.5$. In both cases, the trace plots show stable fluctuations, indicating that the MCMC chains have achieved good mixing, while the autocorrelation plots decrease rapidly, reflecting minimal correlation between consecutive samples. The posterior density plots exhibit distinct peaks, suggesting well-defined parameter estimates. However, for $T = 4.5$, the posterior distributions appear slightly broader compared to $T = 3.8$, implying greater uncertainty in parameter estimates. This difference highlights the influence of sample size and censoring levels on the precision of the Bayesian estimation.

Table 8. ML, MPS, and Bayesian estimation methods for parameters of IPB-XD based on hybrid censored samples: Data II

| $r$ | $T$ | | | Estimates | StEr | Lower | Upper | RF | HRF |
|---|---|---|---|---|---|---|---|---|---|
| 40 | 3.8 | ML | $\alpha$ | 0.20020 | 0.09663 | 0.01081 | 0.38958 | 0.50820 | 0.24399 |
| | | | $\theta$ | 2.35616 | 0.81296 | 0.76277 | 3.94956 | | |
| | | | $\lambda$ | 4.32135 | 1.26104 | 1.84972 | 6.79298 | | |
| | | MPS | $\alpha$ | 0.37421 | 0.16667 | 0.04754 | 0.70088 | 0.51257 | 0.25861 |
| | | | $\theta$ | 1.44124 | 0.39378 | 0.66943 | 2.21305 | | |
| | | | $\lambda$ | 2.93371 | 0.32864 | 2.28958 | 3.57784 | | |
| | | Bayesian | $\alpha$ | 49.93850 | 0.09710 | 49.74671 | 50.12196 | 0.48523 | 0.52356 |
| | | | $\theta$ | 0.32193 | 0.08170 | 0.16057 | 0.47628 | | |
| | | | $\lambda$ | 3.16551 | 1.24930 | 0.59675 | 5.51339 | | |
| | 4.5 | ML | $\alpha$ | 0.33760 | 0.14319 | 0.05694 | 0.61825 | 0.40948 | 0.24641 |
| | | | $\theta$ | 1.70429 | 0.47615 | 0.77103 | 2.63755 | | |
| | | | $\lambda$ | 3.52296 | 0.59317 | 2.36034 | 4.68557 | | |
| | | MPS | $\alpha$ | 0.54149 | 0.21513 | 0.11984 | 0.96314 | 0.41498 | 0.25567 |
| | | | $\theta$ | 1.18796 | 0.27610 | 0.64680 | 1.72912 | | |
| | | | $\lambda$ | 2.79694 | 0.21945 | 2.36682 | 3.22706 | | |
| | | Bayesian | $\alpha$ | 49.93798 | 0.14390 | 49.65375 | 50.20984 | 0.31950 | 0.62666 |
| | | | $\theta$ | 0.32232 | 0.04785 | 0.22781 | 0.41272 | | |
| | | | $\lambda$ | 3.16141 | 0.59348 | 1.95307 | 4.28080 | | |
| 46 | 5.2 | ML | $\alpha$ | 1.93916 | 0.91126 | 0.15308 | 3.72523 | 0.27788 | 0.36784 |
| | | | $\theta$ | 0.72513 | 0.14819 | 0.43467 | 1.01558 | | |
| | | | $\lambda$ | 2.81820 | 0.09739 | 2.62732 | 3.00908 | | |
| | | MPS | $\alpha$ | 3.29888 | 1.67328 | 0.01925 | 6.57851 | 0.28542 | 0.37244 |
| | | | $\theta$ | 0.55135 | 0.10632 | 0.34297 | 0.75973 | | |
| | | | $\lambda$ | 2.66310 | 0.05395 | 2.55736 | 2.76885 | | |
| | | Bayesian | $\alpha$ | 49.92972 | 0.91555 | 48.12043 | 51.65937 | 0.19969 | 0.70107 |
| | | | $\theta$ | 0.32271 | 0.01489 | 0.29328 | 0.35083 | | |
| | | | $\lambda$ | 3.16203 | 0.09745 | 2.96363 | 3.34580 | | |

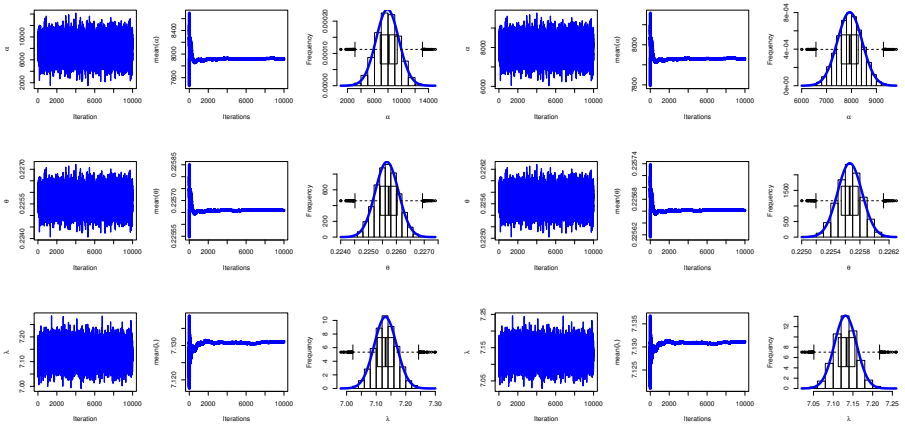

Fig. 9. MCMC plots of Data II

## 7. Concluding remarks

This paper introduces a novel three-parameter extension of the PB-XD, derived through the inverse transformation technique. The resulting IP-BXD offers a versatile framework for modeling non-monotonic behaviors, as it can effectively capture decreasing, increasing, and bathtub-shaped patterns in lifetime data. We provide explicit expressions for key statistical properties, including ordinary moments, QF, incomplete and conditional moments, MRL, and MIT. Additionally, the IP-BXD demonstrates its practical utility in statistical applications through a comprehensive analysis of estimation methods, such as ML and MPS, under complete and hybrid

censoring schemes. Moreover, we delve into the Bayesian estimation framework, employing an informative gamma prior under the squared error loss function. Bayesian credible intervals and ACIs derived from the normal approximation are constructed. A comprehensive Monte Carlo simulation study evaluates the performance of various estimates based on multiple accuracy metrics. To demonstrate the practical utility and versatility of the proposed model, we analyze three real-world datasets and compare its performance against several competing distributions. In addition, we illustrate the application of the proposed methods to real-world scenarios using these data sets. This work is limited to the use of the Bayesian estimating method within MCMC when the loss function is symmetric. Future research can examine how asymmetric loss functions are used in Bayesian estimation. This would offer a more adaptable framework because overestimation and underestimation frequently carry distinct consequences in real-world situations. Furthermore, for computing conditional posteriors, the Tierney-Kadane approximation approach could be used as a productive substitute for computationally demanding MCMC methods.

## References

[1] Burr, I.W. (1942). Cumulative frequency functions. *The Annals of Mathematical Statistics*, *13*(2), 215-232.

[2] Ahmad, K.E., Fakhry, M.E., & Jaheen, Z.F. (1997). Empirical Bayes estimation of P ($Y < X$) and characterizations of Burr-type X model. *Journal of Statistical Planning and Inference*, *64*(2), 297-308.

[3] Surles, J.G., & Padgett, W.J. (2001). Inference for reliability and stress-strength for a scaled Burr type X distribution. *Lifetime Data Analysis*, *7*, 187-200.

[4] Kundu, D., & Raqab, M.Z. (2005). Generalized Rayleigh distribution: different methods of estimations. *Computational Statistics & Data Analysis*, *49*(1), 187-200.

[5] Aludaat, K.M., Alodat, M.T., & Alodat, T.T. (2008). Parameter estimation of Burr type X distribution for grouped data. *Applied Mathematical Sciences*, *2*(9), 415-423.

[6] Fayomi, A., Hassan, A.S., Baaqeel, H., & Almetwally, E.M. (2023). Bayesian inference and data analysis of the unit – power Burr X distribution. *Axioms*, *12*(3), 297.

[7] Usman, R.M., & Ilyas, M. (2020). The power Burr type X distribution: Properties, regression modeling and applications. *Punjab University Journal of Mathematics*, *52*(8).

[8] Abd AL-Fattah, A.M., El-Helbawy, A.A., & Al-Dayian, G.R. (2017). Inverted Kumaraswamy distribution: Properties and estimation. *Pakistan Journal of Statistics*, *33*(1), 37-61.

[9] El Gazar, A.M., Ramadan, D.A., ElGarhy, M., & El-Desouky, B.S. (2025). Estimation of parameters for inverse power Ailamujia and truncated inverse power Ailamujia distributions based on progressive type-II censoring scheme. *Innovation in Statistics and Probability*, *1*(1), 76-87.

[10] Noori, N.A., Abdullah, K.N., & Khaleel, M.A. (2025). Development and applications of a new hybrid Weibull-inverse Weibull distribution. *Modern Journal of Statistics*, *1*(1), 80-103.

[11] Hassan, A.S., & ElMorsey, R. (2019). Parameter estimation for inverted exponentiated Lomax distribution with right censored data. *Gazi University Journal of Science*, *32*(4), 1370-1386.

[12] Ramos, P.L., Louzada, F., Shimizu, T.K., & Luiz, A.O. (2019). The inverse weighted Lindley distribution: Properties, estimation and an application on a failure time data. *Communications in Statistics-Theory and Methods*, *48*(10), 2372-2389.

[13] Guo, L., & Gui, W. (2018). Bayesian and classical estimation of the inverse Pareto distribution and its application to strength-stress models. *American Journal of Mathematical and Management Sciences*, *37*(1), 80-92.

[14] Sharma, V.K., Singh, S.K., Singh, U., & Agiwal, V. (2015). The inverse Lindley distribution: a stress-strength reliability model with application to head and neck cancer data. *Journal of Industrial and Production Engineering*, *32*(3), 162-173.

[15] Barco, K.V.P., Mazucheli, J., & Janeiro, V. (2017). The inverse power Lindley distribution. *Communications in Statistics-Simulation and Computation*, *46*(8), 6308-6323.

[16] Adetunji, A.A., Ademuyiwa, J.A., & Adejumo, O.A. (2020). The inverse Sushila distribution: Properties and application. *Asian Research Journal of Mathematics*, *16*, 28-39.

[17] Okereke, E.W., Gideon, S.N., & Ohakwe, J. (2021). Inverse Akash distribution and its applications. *Scientia Africana*, *20*(2), 61-72.

[18] Lee, S., Noh, Y., & Chung, Y. (2017). Inverted exponentiated Weibull distribution with applications to lifetime data. *Communications for Statistical Applications & Methods*, *24*(3), 227-240.

[19] Hassan, A.S., & Abd-Alla, M. (2019). On the Inverse Power Lomax distribution. *Annals of Data Science*, *6*(2), 259-278.

[20] Enogwe, S.U., Obiora-Ilouno, H.O., & Onyekwere, C.K. (2021). Inverse power Akash probability distribution with applications. *Earthline Journal of Mathematical Sciences*, *6*(1), 1-32.

[21] Yadav, A.S., Maiti, S.S., & Saha, M. (2021). The inverse xgamma distribution: statistical properties and different methods of estimation. *Annals of Data Science*, *8*, 275-293.

[22] Tahir, M.H., Cordeiro, G.M., Ali, S., Dey, S., & Manzoor, A. (2018). The inverted Nadarajah-Haghighi distribution: estimation methods and applications. *Journal of Statistical Computation and Simulation*, *88*(14), 2775-2798.

[23] Hassan, A.S., Elgarhy, M., & Ragab, R. (2020). Statistical properties and estimation of inverted Topp-Leone distribution. *Journal of Statistics Applications & Probability*, *9*(2), 319-331.

[24] Sapkota, L.P., & Kumar, V. (2023). Applications and some characteristics of inverse power Cauchy distribution. *Reliability: Theory & Applications*, *18*(1(72)), 301-315.

[25] Frank, O.I., Obiora-Ilouno, H.O., & Frederick, O.A. (2023). Inverse Hamza distribution: Properties and applications to lifetime data. *Asian Journal of Probability and Statistics*, *23*(1), 46-64.

[26] Almetwally, E.M., & Muhammed, H.Z. (2020). On a bivariate Fréchet distribution. *Journal of Statistics Applications & Probability*, *9*(1), 1-21.

[27] Pokalas, T.M., John, C., Tal, P.P.D., & Johnson, O. (2024). Inverse shanker distribution: Its properties and application. *African Journal of Mathematics and Statistics Studies*, *7*(3), 29-42.

[28] Awajan, M.Y., Ramadan, D.A., & El-Desouky, B.S. (2024). Inverse power modified Chris-Jerry distribution: Properties, estimation, simulation and medical application. *Appl. Math.*, *18*(6), 1261-1271.

[29] Abdelall, Y.Y., Hassan, A.S., & Almetwally, E.M. (2024). A new extention of the odd inverse Weibull-G family of distributions: Bayesian and non-Bayesian estimation with engineering applications. *Computational Journal of Mathematical and Statistical Sciences*, *3*(2), 359-388. DOI: 10.21608/CJMSS.2024.285399.1050.

[30] Louzada, F., Ramos, P.L., & Nascimento, D. (2018). The inverse Nakagami-m distribution: A novel approach in reliability. *IEEE Transactions on Reliability*, *67*(3), 1030-1042.

[31] Omar, M.H., Arafat, S.Y., Hossain, M.P., & Riaz, M. (2021). Inverse maxwell distribution and statistical process control: An efficient approach for monitoring positively skewed process. *Symmetry*, *13*(2), 189.

[32] Al Mutairi, A., Hassan, A.S., Alshqaq, S.S., Alsultan, R., Gemeay, A.M., Nassr, S.G., & Elgarhy, M. (2023). Inverse power Ramos-Louzada distribution with various classical estimation methods and modeling to engineering data. *AIP Advances*, *13*(9), 095117.

[33] Alsadat, N., Elgarhy, M., Karakaya, K., Gemeay, A.M., Chesneau, C., & Abd El-Raouf, M.M. (2023). Inverse unit Teissier distribution: Theory and practical examples. *Axioms*, *12*(5), 502.

[34] Elbatal, I., Hassan, A.S., Gemeay, A.M., Diab, L.S., Ghorbal, A.B., & Elgarhy, M. (2024). Statistical analysis of the inverse power Zeghdoudi model: Estimation, simulation and modeling to engineering and environmental data. *Physica Scripta*, *99*(6), 065231.

[35] Hassan, A.S., Alsadat, N., Chesneau, C., Elgarhy, M., Kayid, M., Nasiru, S., & Gemeay, A.M. (2025). Inverse power XLindley distribution with statistical inference and applications to engineering data. *Scientific Reports*, *15*, 4385. DOI: 10.1038/s41598-025-87023-6.

[36] Ghitany, M.E., Tuan, V.K., & Balakrishnan, N. (2014). Likelihood estimation for a general class of inverse exponentiated distributions based on complete and progressively censored data. *Journal of Statistical Computation and Simulation*, *84*(1), 96-106.

[37] Voda, V.G. (1972). On the inverse Rayleigh distributed random variable. *Reports of Statistical Application Research*, *19*(4), 13-21.

[38] Kenney, F.J., & Keeping. S.E. (1962). *Mathematics of Statistics*. Princeton, NJ.

[39] Moors, J.J.A. (1988). A quantile alternative for kurtosis. *Journal of the Royal Statistical Society: Series D (The Statistician)*, *37*(1), 25-32.

[40] Al Mutairi, A., Khashab, R.H., Almetwally, E.M., Abo-Kasem, O.E., & Ibrahim, G.M. (2023). Bayesian and non-Bayesian inference for inverse Weibull model based on jointly type-II hybrid censoring samples with modeling to physics data. *AIP Advances*, *13*(10).

[41] Haj Ahmad, H., Almetwally, E.M., Rabaiah, A., & Ramadan, D.A. (2023). Statistical analysis of alpha power inverse Weibull distribution under hybrid censored scheme with applications to ball bearings technology and biomedical data. *Symmetry*, *15*(1), 161.

[42] Almetwally, E.M., Alotaibi, R., & Rezk, H. (2023). Estimation and prediction for alpha-power Weibull distribution based on hybrid censoring. *Symmetry*, *15*(9), 1687.

[43] Balakrishnan, N., & Kundu, D. (2013). Hybrid censoring: Models, inferential results and applications. *Computational Statistics & Data Analysis*, *57*(1), 166-209.

[44] Greene, W.H. (2000). *Econometric Analysis*. 4th edn. New York: Prentice-Hall.

[45] Cheng, R.C.H., & Amin, N.A.K. (1983). Estimating parameters in continuous univariate distributions with a shifted origin. *Journal of the Royal Statistical Society: Series B (Methodological)*, *45*(3), 394-403.

[46] Dey, S., Singh, S., Tripathi, Y.M., & Asgharzadeh, A. (2016). Estimation and prediction for a progressively censored generalized inverted exponential distribution. *Statistical Methodology*, *32*, 185-202.

[47] Henningsen, A., & Toomet, O. (2011). maxLik: A package for maximum likelihood estimation in R. *Computational Statistics*, *26*(3), 443-458.

[48] Plummer, M., Best, N., Cowles, K., & Vines, K. (2015). Package 'coda'. http://cran. r-project. org/web/packages/coda/coda. pdf, accessed January, 25, 2015.

[49] El-Sherpieny, E.S.A., Almetwally, E.M., & Muhammed, H.Z. (2020). Progressive type-II hybrid censored schemes based on maximum product spacing with application to power Lomax distribution. *Physica A: Statistical Mechanics and its Applications*, *553*, 124251.

[50] Singh, U., Singh, S.K., & Singh, R.K. (2014). Product spacings as an alternative to likelihood for Bayesian inferences. *Journal of Statistics Applications & Probability*, *3*, 179-188.

[51] Alyami, S.A., Elbatal, I., Alotaibi, N., Almetwally, E.M., & Elgarhy, M. (2022). Modeling to factor productivity of the United Kingdom food chain: Using a new lifetime-generated family of distributions. *Sustainability*, *14*(14), 8942.

[52] De Gusmao, F.R., Ortega, E.M., & Cordeiro, G.M. (2011). The generalized inverse Weibull distribution. *Statistical Papers*, *52*, 591-619.

[53] Muhammad, M., Alshanbari, H.M., Alanzi, A.R., Liu, L., Sami, W., Chesneau, C., & Jamal, F. (2021). A new generator of probability models: the exponentiated sine-G family for lifetime studies. *Entropy*, *23*(11), 1394.

[54] Okoli, O.M., Osuji, G.A., & Onyekwere, C.K. (2021). Generalized inverse power Sujatha distribution with applications. *Asian Journal of Probability and Statistics*, *15*(3), 11-25.

[55] Gacula Jr, M.C., & Kubala, J.J. (1975). Statistical models for shelf life failures. *Journal of Food Science*, 40(2), 404-409.

[56] Elbatal, I., Alotaibi, N., Almetwally, E.M., Alyami, S.A., & Elgarhy, M. (2022). On odd perks-G class of distributions: properties, regression model, discretization, Bayesian and non-Bayesian estimation, and applications. *Symmetry*, *14*(5), 883.

[57] Suhaila, J., Deni, S.M., Wan Zin, W.Z., & Jemain, A.A. (2010). Spatial patterns and trends of daily rainfall regime in Peninsular Malaysia during the southwest and northeast monsoons: 1975-2004. *Meteorology and Atmospheric Physics*, *110*, 1-18.